1 Introduction

Cold collisionless fluid that explains many observations in astrophysics and cosmology. It's existence shouldn't be questioned, only its microphysical constitution.

1.1 Evidence for Dark Matter

Today, the amount of evidence in support of dark matter's existence is overwhelming. This evidence comes from astrophysical and cosmological observations that are inconsistent with a universe composed entirely of visible matter. This section reviews this evidence.

1.1.1 Astrophysical Observations

Galaxy Clusters

Some of the first hints for the existence of dark matter came from observations of galaxy clusters. Perhaps the most famous analysis was performed by Fritz Zwicky [1], who was puzzled by the high rotational velocities of galaxies within the Coma Cluster. By applying the virial theorem, equating the cluster's kinetic and gravitational potential energies, he found that the cluster would need to contain a much more significant amount of *dunkle materie* (dark matter) than visible matter to accommodate these high velocities.

Rotation Curves of Spiral Galaxies

The anomalous rotational velocities observed in galaxy clusters can also be observed at the galactic scale. The rotation curves of spiral galaxies, which relate the rotational velocities of stars to their distance from the galactic centre, were observed to be flat at large distances. From the observed distribution of visible matter, Newtonian mechanics predicts that the orbital velocity of a star a distance r from the galactic centre, $v_\star(r)$, is related to the mass contained within a radius r, $M(r)$, through

$$v_\star(r) = \sqrt{\frac{GM(r)}{r}}, \tag{1.1}$$

indicating that the velocity should fall off as $1/\sqrt{r}$ at the outer regions of the galaxy where $M(r)$ is constant. Instead, observations of many spiral galaxies indicate that this velocity remains constant out to the galaxy's edge.

A simple way to produce such a rotation curve is to introduce a spherically symmetric distribution of dark matter surrounding the galaxy,

$$\rho_{\mathrm{DM}}(r) = \frac{v_0^2}{4\pi G r^2}, \tag{1.2}$$

which results in a constant rotational velocity of v_0 out to the galaxy edge. Detailed simulations of structure formation in a Cold Dark Matter (CDM) Universe indicate that the true distribution is better represented by distribution functions such as the Navaro-Frenk-White (NFW) profile [2, 3] or Einasto [4] profiles, which are commonly used in the literature.

An example rotation curve for galaxy NGC 6503 is presented in Fig. 1.1, with the contributions from each of the matter components to the rotational velocity shown [5, 6]. As can be seen, the visible matter constituting disk and gas components does not explain the observed rotational velocity.

Gravitational Lensing

As described by General Relativity, the curvature of space-time around massive entities causes light to travel along curved paths. As such, the mass of astrophysical structures can be deduced from the extent to which they distort the images of objects in the background. The extent of the distortions depends on how massive the foreground object is, ranging from the shearing of the background image (weak lensing), to multiple copies of the background object appearing (strong lensing) [7]. The disparity between the mass obtained from gravitational lensing and the mass of visible matter in the system is further evidence of dark matter's existence [8, 9].

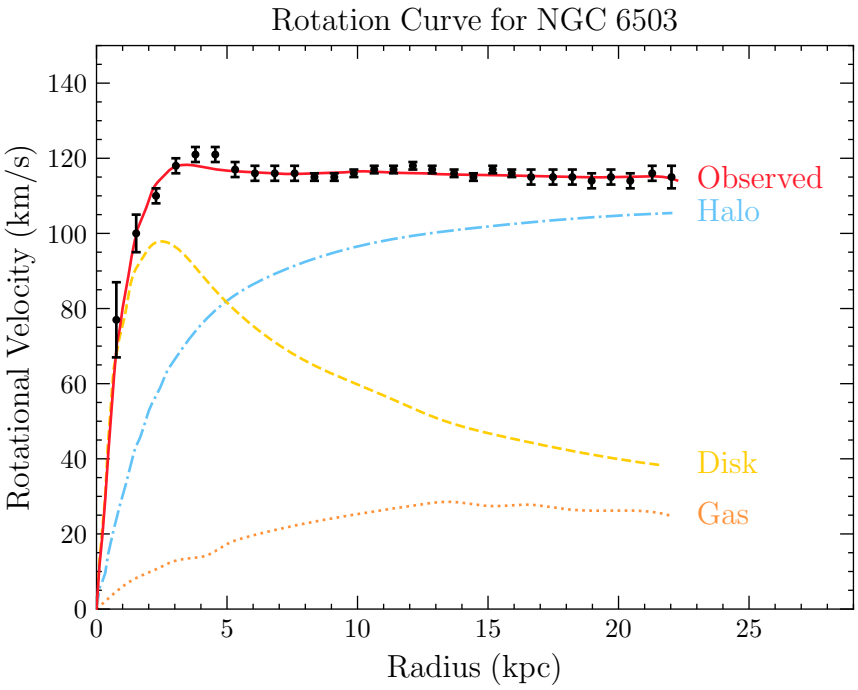

Figure 1.1: Galaxy rotation curve for NGC 6503, showing the contributions to the total velocity (red) from the DM halo (blue), disk (yellow), and gas components. Data used in making this plot was obtained from [5, 6].

The Bullet Cluster

Galaxy cluster 1E 0657-56, commonly referred to as the "bullet cluster", was formed by the collision of two separate galaxy clusters. The baryonic matter in these clusters is mostly composed of a strongly interacting gas and, as expected, produced a significant amount of X-rays during the collision. These X-rays were imaged by the Chandra X-Ray telescope [10], providing information on the resulting distribution of the visible matter. This is shown by the red regions of Fig. 1.2, where it can be seen how the visible matter has been smeared due to the collision. However, when the gravitational potential was mapped using gravitational lensing, it was clear that the majority of the mass was displaced relative to the visible matter. This mass is attributed to the dark matter components of the original clusters. As indicated by the purple regions in Fig. 1.2, the dark matter halos seem to have passed through each other mostly unperturbed. This tells us that not only is the majority of the mass comprised of dark matter, but that the dark matter has extremely weak interactions with both the visible matter and itself.

Figure 1.2: Image of the Bullet Cluster with contours of the gravitational potential superposed. The red regions indicate the baryonic matter after the collision, while the purple regions are the expected DM components deduced from gravitational lensing. [10, 11]

1.1.2 Cosmological Evidence

The current best cosmological model is the Λ-Cold Dark Matter model (ΛCDM), in which Λ refers to the cosmological constant associated with dark energy, and as the name suggests, cold (i.e. non-relativistic) dark matter plays a prominent role. The key components of this model are the aforementioned dark energy and dark matter, along with baryonic matter, and it assumes that gravity is described by Einstein's General Relativity. The total energy density of the universe, $\rho_{\text{Univ.}}$, can be broken down into three components based on how their density redshifts with the expansion of the Universe. In the ΛCDM model, these components are matter, radiation, and the vacuum energy Λ. The cosmological abundances of each component, (Ω_{m}, Ω_{r}, Ω_Λ respectively), are expressed as a fraction of the critical density, ρ_{crit},

$$\rho_{\text{crit}} = \frac{H^2}{8\pi G_N}, \tag{1.3}$$

$$\Omega_i = \frac{\rho_i}{\rho_{\text{crit}}}, \tag{1.4}$$

where H is the Hubble parameter, such that the total energy density of the Universe satisfies

$$\Omega_{\rm m} + \Omega_{\rm r} + \Omega_{\Lambda} = \frac{\rho_{\rm Univ.}}{\rho_{\rm crit}}. \tag{1.5}$$

The ratio $\rho_{\rm Univ.}/\rho_{\rm crit}$ determines the curvature of the universe, with values greater than 1 corresponding to a closed universe, less than 1 to an open universe, and equal to 1 to a spatially flat universe. Current observations are consistent with a spatially flat universe, and so we have $\sum_i \Omega_i = 1$.

The ΛCDM model has seen huge success as it provides explanations for observed the power spectrum of the Cosmic Microwave Background (CMB), the large-scale structure of the Universe, the abundances of light elements (hydrogen, deuterium, helium, and lithium), and the accelerated expansion rate of the Universe. These observations constrain the parameters of the model and hence provide a complimentary probe of the properties of dark matter to the astronomical observations discussed above.

The Cosmic Microwave Background

One of the strongest probes of cosmological models is the Cosmic Microwave Background (CMB), relic photons from the time epoch of last scattering. This occurred after recombination, at a temperature of around $\sim 3000\,\mathrm{K}$, once the photons had decoupled from the baryonic matter and could freely propagate through the universe. The photons observed today have been redshifted by the expansion of the Universe and are well described by a blackbody spectrum with a temperature of $T_{\rm CMB} = 2.73 \pm 0.0006\,\mathrm{K}$. Observations of the CMB temperature reveal that it is not exactly isotropic, with anisotropies at the level of $\delta T_{\rm CMB}/T_{\rm CMB} \sim 10^{-5} - 10^{-6}$ seen on a range of angular scales in the sky. These anisotropies were seeded by the primordial density perturbations that arise during inflation. These perturbations evolve due to the acoustic oscillations of the photon-baryon plasma driven by the interplay between the pressure from the photons and the gravitational attraction of the matter. The oscillations cease once the photons decouple, freezing in their temporal phases that are observed as peaks in the angular power spectrum of the temperature anisotropies.

Measurements of the CMB power spectrum provide information on many of the cosmological parameters. The locations of the acoustic peaks depend on the spatial geometry of the Universe and hence constrains $\Omega_{\rm tot}$. The total matter density, $\Omega_{\rm m}$, affects how the CMB spectrum is gravitationally lensed. The relative amplitudes of the peaks probe the baryon-to-photon ratio and hence the baryon density, $\Omega_{\rm b}$. Finally, the density of dark matter, $\Omega_{\rm DM}$, is obtained by fitting the cosmological parameters to the exact shape of the spectrum [5, 12].

The Planck collaboration most recently performed a precise measurement of the CMB power spectrum in 2018, obtaining best-fit parameters [12, 13]

$$\Omega_{\mathrm{m}} = 0.311 \pm 0.006, \quad \Omega_{\Lambda} = 0.689 \pm 0.006, \tag{1.6}$$

for the matter and dark energy densities. They obtained a total energy density of $\Omega_{\mathrm{tot}} = 1.011 \pm 0.006$ at 68% confidence level, providing strong evidence for a spatially flat Universe. The breakdown of the matter density into the dark and baryonic components is determined by combining the CMB results with constraints from Big Bang Nucleosynthesis (BBN)[1] giving

$$\Omega_{\mathrm{DM}} h^2 = 0.1193 \pm 0.0009, \quad \Omega_{\mathrm{b}} h^2 = 0.02242 \pm 0.00014, \tag{1.7}$$

where h is the dimensionless Hubble constant such that the Hubble parameter today is $H_0 = 100\, h\, \mathrm{km\, s^{-1}}$ Mpc.

Large Scale Structure

After recombination, the pressure on the baryonic matter from photons began to decrease, eventually allowing the small density perturbations to grow. This led to the growth of stars, galaxies, and the large-scale structure we observe today [14]. N-body simulations of the Universe's evolution require a cold dark matter component for this structure to form. While a small component of the dark matter can be warm, hot dark matter would wash out small-scale structures [15].

1.2 Potential Models of Dark Matter

Given that baryonic matter is composed of particles described by the Standard Model (SM) of particle physics, it is a fair assumption that dark matter will also have a particle nature. Therefore, models of particle dark matter are built by extending the SM in a way consistent with its symmetries. Such models may be as simple as introducing a single new field into the SM, or there may be a more extensive hidden sector with a complicated symmetry structure. Additionally, there are compelling theories in which dark matter is not a fundamental particle, such as primordial black holes (PBHs) formed in the early universe. Given the few details we know about dark matter, there exists an enormous library of viable dark matter candidates. However, there are generic properties a good dark matter candidate must satisfy, namely:

[1] BBN is the process that produced the light elements (D, ^{3}He, ^{4}He, and ^{7}Li) were produced in the early universe. This process is highly sensitive to the physical condition of the universe at that time, allowing for strong constraints to be placed on physics beyond the Standard Model.

- **Stable on Cosmological Timescales:** Dark matter must either be stable or have a lifetime significantly longer than the age of the Universe to be present in its current abundance.
- **Neutral or milli-charged under Electromagnetism:** Dark matter, as its name suggests, does not significantly interact with light. Requiring that dark matter be completely decoupled from the Standard Model plasma by the time of recombination yields an upper bound on the electric charge of dark matter [16]

$$q_{\mathrm{DM}}/e < \begin{cases} 3.5 \times 10^{-7} \left(\frac{m_{\mathrm{DM}}}{1\,\mathrm{GeV}}\right)^{0.58}, & m_{\mathrm{DM}} > 1\,\mathrm{GeV} \\ 4.0 \times 10^{-7} \left(\frac{m_{\mathrm{DM}}}{1\,\mathrm{GeV}}\right)^{0.35}, & m_{\mathrm{DM}} < 1\,\mathrm{GeV} \end{cases} \tag{1.8}$$

- **Small Self-Interactions:** The standard ΛCDM cosmology assumes that the dark matter is collisionless. However, small dark matter self-interactions can help resolve existing small-scale structure issues [17, 18]. Current limits on the self-interaction cross-section are $\sigma_{\mathrm{DM-DM}}/m_{\mathrm{DM}} < 0.48\,\mathrm{cm}^2/\mathrm{g}$ come from merging galaxy clusters [11] and the ellipticity of galaxies obtained from X-ray observations [19].
- **Cold:** Dark matter is required to be non-relativistic at the time of structure formation. At most, a small component of the dark matter can be warm (semi-relativistic).

A selection of the more prominent dark matter candidates is shown in Fig. 1.3. The key features of a few of these models are discussed below.

WIMPs

Weakly Interacting Massive Particles (WIMPs) are a class of dark matter candidates that generically have masses and interaction strengths around the weak scale. Many extensions of the SM naturally predict the existence of such a particle, with famous examples being the lightest supersymmetric particle in supersymmetric theories [21], or the lightest stable Kaluza-Klein mode in theories with extra dimensions [22].

Nowadays, WIMP dark matter is used almost synonymously to mean thermal relic, referring to a species whose relic abundance is produced thermally in the early universe through the freeze-out mechanism [23]. In this paradigm, the WIMP is initially in thermal equilibrium with the Standard Model bath. This equilibrium is maintained as long as the interaction rates of the WIMP with the bath, denoted Γ, remain faster than the Hubble expansion of the universe, H. As the universe continues to expand, the temperature of the bath drops, slowing down the interaction

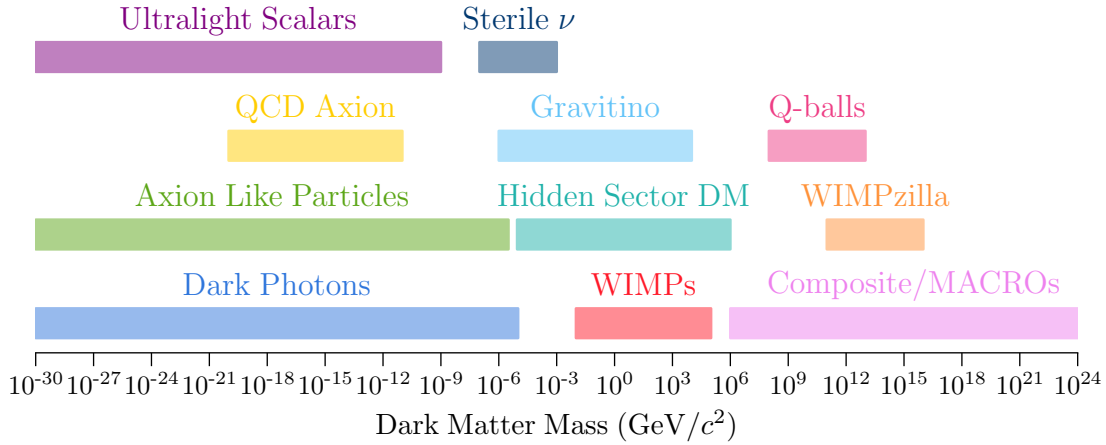

Figure 1.3: Illustrative landscape of dark matter models and the mass range for which they predict a valid candidate. Details can be found in the Dark Matter chapter of the PDG [20].

rates. Eventually, the expansion rate overtakes the interaction rates, $\Gamma/H \lesssim 1$, and the interactions "freeze out" causing the WIMP to fall out of equilibrium with the bath. At this point, the WIMPs can no longer efficiently annihilate, and their abundance gets "frozen-in" to the value it had at freeze-out, leading to the abundance observed today.

A cold thermal relic, such as dark matter, will freeze out after it has become non-relativistic. In this scenario, the interaction rates become Boltzmann suppressed[2], and the species rapidly freezes out. The relic density is therefore sensitive to the annihilation cross-section of the species, $\langle \sigma_{\text{ann}} v \rangle$. More efficient annihilations correspond to larger cross-sections, resulting in the species remaining in equilibrium for longer times. This allows the number density to continue following the exponentially decreasing Boltzmann distribution and yield a smaller relic abundance. The evolution of the abundance of a Majorana fermion WIMP of mass $m_{\text{WIMP}} = 100\,\text{GeV}$ is shown in Fig. 1.4 for three values of the annihilation cross-section. A simple expression relating the annihilation cross-section and the

[2]The number density of a non-relativistic species in thermal equilibrium with the bath will follow $n \propto (mT_{\text{bath}})^{3/2} \exp(-m/T_{\text{bath}})$. Once the temperature falls below the mass of the species, the number density becomes exponentially suppressed. This is what is known as "Boltzmann suppression".

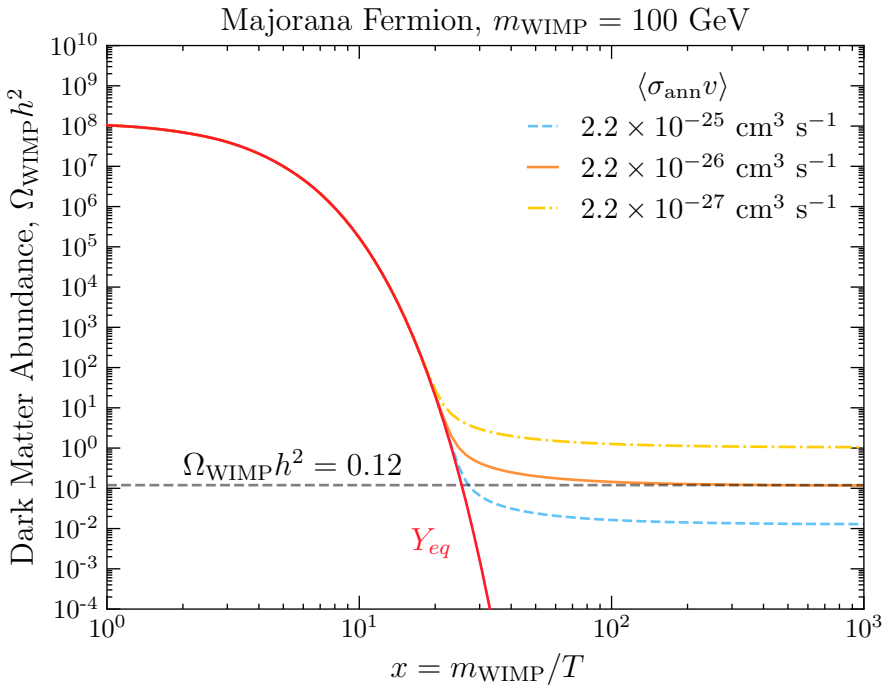

Figure 1.4: Evolution of the DM abundance as a function of $x = m_{\rm DM}/T$. The red line tracks the abundance of the WIMP if it remains in equilibrium with the bath. The relic abundance for three different annihilation cross-sections is shown in blue, orange, and yellow for $\langle\sigma_{\rm ann}v\rangle = 2.2 \times 10^{-25}$, 2.2×10^{-26}, and 2.2×10^{-27} cm^{3}s^{-1} respectively.

abundance that is correct to $\sim 5\%$ can be obtained [24]

$$\Omega_{\rm DM}h^2 = \frac{10^{-27}\,{\rm cm}^3\,{\rm s}^{-1}}{\langle\sigma_{\rm ann}v_\chi\rangle}\frac{x_*}{g_*^{1/2}} \tag{1.9}$$

$$\sim 0.12\left(\frac{2.2\times10^{-26}\,{\rm cm}^3\,{\rm s}^{-1}}{\langle\sigma v\rangle}\right), \quad m_\chi \gtrsim 10\,{\rm GeV}, \tag{1.10}$$

where $x_* = m_{\rm WIMP}/T_*$ is evaluated at an intermediate temperature between equilibrium and freeze-out, with g_* the effective number of relativistic degrees of freedom present at this time.

The allowed mass range for a thermal WIMP is between $10\,{\rm MeV} \lesssim m_{\rm WIMP} \lesssim 100\,{\rm TeV}$. Lighter WIMPs will make non-negligible contributions to the effective number of neutrinos at the time of Big Bang Nucleosynthesis, measured to be $N_{eff}^{\rm BBN} = 3.044$ [25], altering the observed abundances of the light elements. The CMB offers an additional probe of $N_{\rm eff}$ at the later time of recombination and can be combined with the BBN result leading to the value $N_{eff} = 2.99 \pm 0.17$ [12].

Given the Standard Model predicts a value of $N_{\text{eff}} = 3.044$, contributions from additional relativistic degrees of freedom must be less than $\Delta N_{\text{eff}} < 0.28$ [25]. At the high end of this range, masses larger than $\sim 100\,\text{TeV}$ are excluded from partial wave unitarity [26].

Axions

The axion originally arose from the Pecci-Quinn solution to the Strong CP problem. This refers to the lack of observed CP-violation in the QCD sector of the Standard Model that arises from the topological term in the Lagrangian

$$\mathcal{L}_{\theta_{\text{QCD}}} = \frac{g_s^2}{32\pi}\theta_{\text{QCD}} G_{\mu\nu}\tilde{G}^{\mu\nu}, \tag{1.11}$$

where g_s is the QCD coupling constant, $G_{\mu\nu}$ is the gluon field strength tensor and $\tilde{G}^{\mu\nu}$ is its dual. This term generates an electric dipole moment for the neutron (nEDM) that has yet to be observed experimentally. The current upper bound on the nEDM is $|d_n| < 0.18 \times 10^{-26}\, e\,\text{cm}$ [27] and can be translated to an upper bound on the CP-violating QCD θ-parameter such that $|\theta_{QCD}| \lesssim 10^{-10}$, raising questions as to why this value seems to be fine-tuned to such a small value.

The Peccei-Quinn solution to this problem introduces a new, anomalous, global $U(1)_{\text{PQ}}$ symmetry and promotes θ_{QCD} to be a dynamical field. Wilczck [28] and Weinberg [29] showed that the axion emerges as the pseudo-Goldstone boson associated with the breaking of $U(1)_{\text{PQ}}$. Though the original axion was quickly out, many modern extensions of the SM predict the existence of a QCD axion. Two of the most prominent UV completions of the axion are the KSVZ [30, 31] and DFSZ [32, 33] models. In these models, the axion produced in the early Universe can serve the role of cold dark matter today. This makes it a very compelling dark matter candidate, as it solves two of the biggest mysteries of physics in one neat package.

However, solving the Strong CP problem can be rather restrictive on the model parameters. For example, the QCD axion's coupling to the photon, $g_{a\gamma\gamma}$, is not a free parameter and depends on the scale at which the PQ symmetry is broken. Many models introduce a light pseudoscalar particle, say a, that couples to the photon in the same way as the QCD axion,

$$\mathcal{L}_{a\gamma\gamma} = -\frac{g_{a\gamma\gamma}}{4} a F_{\mu\nu}\tilde{F}^{\mu\nu}, \tag{1.12}$$

but is not associated with a solution to the Strong CP problem. Such pseudoscalars are known as "Axion Like Particles" (ALPs) and can make a good dark matter candidate.

Primordial Black Holes

Primordial black holes (PBHs) are formed during the early Universe through various mechanisms. The simplest mechanism predicts that PBHs are produced from the gravitational collapse of superhorizon density fluctuations seeded during inflation [34–36]. Unlike black holes that originate from stellar collapse, which have masses $\gtrsim 3M_\odot$, the mass of a PBH can be arbitrary. PBHs can also make a good dark matter candidate, satisfying all the criteria points outlined above. In fact, PBHs with a mass between $\sim (10^{-17} - 10^{-12})\ M_\odot$, dubbed "asteroid mass PBHs", can account for 100% of the dark matter content in the Universe [37]. Outside this range, PBHs can still make up a small fraction of dark matter [38].

1.2.1 Dark Matter in an Effective Fields Theory Framework

For a dark matter candidate to be truly compelling, it should be able to be embedded into an ultraviolet (UV) complete theory. Such theories are renormalisable[3] and gauge invariant under the SM gauge group $SU(3)_{\text{colour}} \otimes SU(2)_L \otimes U(1)_Y$. This allows them to be predictive up to arbitrarily high energies. These theories are typically quite complex, requiring the introduction of multiple new fields and many more free parameters. As an example, consider the phenomenological Minimal Supersymmetric Standard Model (pMSSM) [38] in which the lightest neutralino[4] can be a thermal WIMP dark matter candidate. In this theory, 19 free parameters are introduced on top of the free parameters in the SM, requiring 38 independent experimental observations to fully constrain the model. Given that at this time, all good dark matter candidates are equally likely to be the correct one, a model-independent approach to interpreting experimental results is desirable. This is achieved by describing the interactions of dark matter with the SM through an effective field theory (EFT).

1.2.2 Overview of Effective Field Theory

Modern physics can be thought of as a ladder of theories that are designed to describe the physics present at a given energy (or length) scale. For example, Newtonian mechanics is a sufficient description of the physics experienced in our everyday lives. However, in situations where the energy is comparable to the mass of the system, Newtonian mechanics breaks down, and Special Relativity must be

[3] In a renormalisable theory, the infinities that arise from UV divergences can be absorbed by fixing a finite number of parameters to experimentally observed values.

[4] The neutralinos are the mass eigenstates of the supersymmetric partners of the neutral gauge bosons and the higgsino.

used to describe the physics. In particle physics, the Standard Model provides an excellent description of particle interactions up to the energies reached at LHC, 13.6 TeV, and perhaps even further beyond. However, even it is expected to break down at higher energy scales, in particular at the Planck scale, where a quantum theory of gravity is required. Hence, both Newtonian mechanics and the SM are low-energy, effective descriptions of a more complete theory.

This philosophy based on only describing the physics relevant below some energy scale, Λ, is the core principle of EFTs. The Lagrangian for the effective theory only contains the degrees of freedom that can be produced below the scale Λ, i.e. fields that have masses less than this scale. This low-energy regime described by the EFT is often called the infrared (IR) regime.

In general, the EFT Lagrangian will contain renormalizable terms, $\mathcal{L}_{\text{renorm.}}$, built out of operators that have mass dimension ≤ 4, as well as operators with mass dimension $n > 4$, $\mathcal{O}_i^{(n)}$, that encapsulate the contributions from the UV physics. Each of these higher dimensional operators will be suppressed by the scale of new physics, Λ^{4-n}. The effective Lagrangian can then be written as

$$\mathcal{L}_{\text{EFT}} = \mathcal{L}_{\text{renorm.}} + \sum_{n>4} \sum_{i=1}^{j_n} \frac{C_i^{(n)}(\tilde{\mu})}{\Lambda^{n-4}} \mathcal{O}_i^{(n)}, \tag{1.13}$$

where we sum over all j_n operators present at mass dimension n. The expansion coefficients, $C_i^{(n)}$, are the Wilson coefficients that contain the effects of the UV physics. In general, the Wilson coefficients run with the energy scale they are evaluated at, $\tilde{\mu}$, described by the renormalisation group equations (RGEs). The sum over the mass dimension of the operators is typically terminated at some sensible value, as higher dimensional operators get increasingly suppressed by the cutoff scale Λ.

The series of operators in Eq. 1.13 can be constructed in two different ways. First, we assume some prior knowledge of the underlying UV theory. Then, for a given energy scale Λ, the heavy degrees of freedom are known, and can be explicitly integrated out. There are various methods for performing this process, the simplest being expanding the propagator of the heavy fields in powers of the momenta over the heavy mass, $(p/M)^2$. For the simple case of a heavy scalar, this corresponds to

$$\frac{i}{p^2 - M^2} = \frac{-i}{M^2} \left(\frac{1}{1 - (p/M)^2} \right) \approx \frac{-i}{M^2} \left(1 + \left(\frac{p}{M} \right)^2 + \mathcal{O}\left(\left(\frac{p}{M} \right)^4 \right) \right). \tag{1.14}$$

An alternate method is to replace the heavy fields in the Lagrangian with their classical equations of motion. The resulting effective Lagrangian will contain all the operators generated by the UV theory at tree level. Constructing an EFT in this way is called the *top-down* method.

The second method of constructing an EFT is to be agnostic to the UV physics and write down all possible operators that can be constructed from the IR degrees of freedom. These operators must obey the symmetries of the IR theory, as well as any other constraints one wishes to impose[5]. This is the *bottom-up* approach, offering a more model-independent approach than the top-down method. The Wilson coefficients, in this case, will be arbitrary functions of the energy scale determined by solving the RGEs.

In general, the parameter space of the EFT will be lower dimensional than those of the corresponding UV models. This allows for an easier comparison with experimental results, as fewer parameters need to be fit to the data. Once the Wilson coefficients have been constrained at the low energy scale of the experiments, they can be matched to the coefficients generated by some UV theory at another scale, thereby constraining the UV parameters.

1.2.3 Dimension 6 EFT Operators for Dirac Fermion Dark Matter

This work will focus on dimension 6 EFT operators that describe the interactions of Dirac fermion dark matter with standard model fermions. These operators will have a structure

$$\mathcal{L}^{(6)}_{\text{EFT}} \sim \frac{1}{\Lambda^2}(\bar{\chi}\Gamma_{\text{DM}}\chi)(\bar{f}\Gamma_{\text{SM}}f), \tag{1.15}$$

where the Γ_i determines the Lorentz structure of the interaction by taking appropriate combinations from the set

$$\Gamma_i \in \{1, i\gamma_5, \gamma^\mu, i\gamma^\mu\gamma^5, \sigma^{\mu\nu}, i\sigma^{\mu\nu}\gamma^5\}. \tag{1.16}$$

For example, the case of $\Gamma_\chi = \Gamma_{\text{SM}} = 1$ yields scalar currents for both the DM and SM fermions and would correspond to integrating out a heavy scalar mediator in the UV theory. Under the assumption of minimal flavour violation (MFV)[6] are ten such operators at dimension six that form a linearly independent basis. These are given in Table 1.1, along with spin-averaged squared matrix element for dark matter scattering with a fermion. The operators are classified based on the Lorentz nature of the SM fermion bilinear; D1-2: Scalar (S), D3-4: Pseudoscalar (P), D5-6: Vector (V), D7-8: Axial-vector (A), and D9-10: tensor (T). The coupling constant, g_f, for operators that involve the S and P fermion bilinears (operators D1-4) are

[5]For example, one might require that no flavour changing processes are present at dimension 5, despite such operator being allowed by the symmetries.

[6]MFV is the assumption that the only source of flavour violation in the quark sector comes from the SM Yukawa matrices and not from any new physics introduced at a higher scale.

Name	Operator	g_f	$\lvert\overline{M}(s,t,m_i)\rvert^2$
D1	$\bar{\chi}\chi\ \bar{f}f$	$\frac{y_f}{\Lambda_f^2}$	$g_f^2\frac{\left(4m_\chi^2-t\right)\left(4m_\chi^2-\mu^2 t\right)}{\mu^2}$
D2	$\bar{\chi}\gamma^5\chi\ \bar{f}f$	$i\frac{y_f}{\Lambda_f^2}$	$g_f^2\frac{t\left(\mu^2 t-4m_\chi^2\right)}{\mu^2}$
D3	$\bar{\chi}\chi\ \bar{f}\gamma^5 f$	$i\frac{y_f}{\Lambda_f^2}$	$g_f^2 t\left(t-4m_\chi^2\right)$
D4	$\bar{\chi}\gamma^5\chi\ \bar{f}\gamma^5 f$	$\frac{y_f}{\Lambda_f^2}$	$g_f^2 t^2$
D5	$\bar{\chi}\gamma_\mu\chi\ \bar{f}\gamma^\mu f$	$\frac{1}{\Lambda_f^2}$	$2g_f^2\frac{2\left(\mu^2+1\right)^2 m_\chi^4-4\left(\mu^2+1\right)\mu^2 s m_\chi^2+\mu^4\left(2s^2+2st+t^2\right)}{\mu^4}$
D6	$\bar{\chi}\gamma_\mu\gamma^5\chi\ \bar{f}\gamma^\mu f$	$\frac{1}{\Lambda_f^2}$	$2g_f^2\frac{2\left(\mu^2-1\right)^2 m_\chi^4-4\mu^2 m_\chi^2\left(\mu^2 s+s+\mu^2 t\right)+\mu^4\left(2s^2+2st+t^2\right)}{\mu^4}$
D7	$\bar{\chi}\gamma_\mu\chi\ \bar{f}\gamma^\mu\gamma^5 f$	$\frac{1}{\Lambda_f^2}$	$2g_f^2\frac{2\left(\mu^2-1\right)^2 m_\chi^4-4\mu^2 m_\chi^2\left(\mu^2 s+s+t\right)+\mu^4\left(2s^2+2st+t^2\right)}{\mu^4}$
D8	$\bar{\chi}\gamma_\mu\gamma^5\chi\ \bar{f}\gamma^\mu\gamma^5 f$	$\frac{1}{\Lambda_f^2}$	$2g_f^2\frac{2\left(\mu^4+10\mu^2+1\right)m_\chi^4-4\left(\mu^2+1\right)\mu^2 m_\chi^2(s+t)+\mu^4\left(2s^2+2st+t^2\right)}{\mu^4}$
D9	$\bar{\chi}\sigma_{\mu\nu}\chi\ \bar{f}\sigma^{\mu\nu}f$	$\frac{1}{\Lambda_f^2}$	$8g_f^2\frac{4\left(\mu^4+4\mu^2+1\right)m_\chi^4-2\left(\mu^2+1\right)\mu^2 m_\chi^2(4s+t)+\mu^4(2s+t)^2}{\mu^4}$
D10	$\bar{\chi}\sigma_{\mu\nu}\gamma^5\chi\ \bar{f}\sigma^{\mu\nu}f$	$\frac{i}{\Lambda_f^2}$	$8g_f^2\frac{4\left(\mu^2-1\right)^2 m_\chi^4-2\left(\mu^2+1\right)\mu^2 m_\chi^2(4s+t)+\mu^4(2s+t)^2}{\mu^4}$

Table 1.1: Dimension 6 EFT operators [39] for the coupling of Dirac DM to fermions (column 2), together with the squared matrix elements DM-fermion scattering (column 5), where s and t are Mandelstam variables, $\mu = m_\chi/m_T$, and m_T is the target mass.

normalised by the corresponding Yukawa couplings. This is because, in a UV complete theory, these bilinears would couple to the new scalar/pseudoscalar field that mediates the interactions with the dark matter. In many models, this new field will mix with the SM Higgs field, leading to couplings that depend on the fermion masses. The remaining bilinears have coupling constants that depend only on the cutoff scale, Λ_f.

1.2.4 From DM-Quark to DM-Nucleon Interactions

The operators in Table 1.1 describe dark matter interactions at the quark level, as these are the degrees of freedom most models are formulated with. However, we will primarily be interested in dark matter scattering with baryons, which requires taking the matrix element of the quark operators between baryon states, i.e. $\langle\mathcal{B}|\bar{q}\,\Gamma_q q|\mathcal{B}\rangle$. These matrix elements can be calculated through the application of Chiral Perturbation Theory (ChPT), giving a baryon level EFT. The operators of this EFT will have the same form as those in Table 1.1, with the obvious re-

placement of $f \to \mathcal{B}$, as well as additional form factors that take into account the structure of the baryons.

The required form factors for each operator have been calculated at zero momentum transfer in Ref. [40] and are given by

$$c_{\mathcal{B}}^{S}(0) = \frac{2m_{\mathcal{B}}^2}{v^2}\left[\sum_{q=u,d,s} f_{T_q}^{(\mathcal{B})} + \frac{2}{9} f_{T_G}^{(\mathcal{B})}\right]^2, \tag{1.17}$$

$$c_{\mathcal{B}}^{P}(0) = \frac{2m_{\mathcal{B}}^2}{v^2}\left[\sum_{q=u,d,s} \left(1 - 3\frac{\overline{m}}{m_q}\right)\Delta_q^{(\mathcal{B})}\right]^2, \tag{1.18}$$

$$c_{\mathcal{B}}^{V}(0) = 9, \tag{1.19}$$

$$c_{\mathcal{B}}^{A}(0) = \left[\sum_{q=u,d,s} \Delta_q^{(\mathcal{B})}\right]^2, \tag{1.20}$$

$$c_{\mathcal{B}}^{T}(0) = \left[\sum_{q=u,d,s} \delta_q^{(\mathcal{B})}\right]^2, \tag{1.21}$$

where $v = 246$ GeV is the vacuum expectation value of the SM Higgs field, $\mathcal{B}$ is the baryonic species, $\overline{m} \equiv (1/m_u + 1/m_d + 1/m_s)^{-1}$ and $f_{T_q}^{(\mathcal{B})}$, $f_{T_G}^{(\mathcal{B})} = 1 - \sum_{q=u,d,s} f_{T_q}^{(\mathcal{B})}$, $\Delta_q^{(\mathcal{B})}$ and $\delta_q^{(\mathcal{B})}$ are the hadronic matrix elements, determined either experimentally or by lattice QCD simulations[7]. The specific values of these matrix elements for various baryons are provided in Appendix **ADD APPENDIX**.

The assumption of zero-momentum transfer is valid when considering interactions with momentum transfers $\lesssim 1\,\text{GeV}$, such as in direct detection experiments. Once the momentum transfer exceeds this, the internal structure of the baryon begins to be resolved, and an additional momentum-dependent form factor is required to account for this [41],

$$F_{\mathcal{B}}(t) = \frac{1}{(1 - t/Q_0)^2}, \tag{1.22}$$

where t is the Mandelstam variable, and Q_0 is an energy scale that depends on the hadronic form factor. For simplicity, we will conservatively take $Q_0 = 1\,\text{GeV}$ for all operators. Putting everything together, the squared coupling constants for dark matter-baryon interactions are obtained by making the replacement

$$g_f^2 \to \frac{c_{\mathcal{B}}^{I}(t)}{\Lambda_q^4} \equiv \frac{1}{\Lambda_q^4} c_{\mathcal{B}}^{I}(0) F_{\mathcal{B}}^2(t), \quad I \in S, P, V, A, T, \tag{1.23}$$

[7] The superscript letters S, P, V, A and T stand for Scalar, Pseudoscalar, Vector, Axial-vector and Tensor interactions respectively. The corresponding operators are: D1-2 for S; D3-4 for P; D5-6 for V, D7-8 for A; and D9-10 for T.

in the matrix elements in the final column of Table 1.1.

1.3 Current Status of Dark Matter Constraints

In broad terms, there are three main ways that we can search for evidence of dark matter, often termed "make it, shake it, or break it". "Make it" refers to the production of dark matter at colliders; "break it" to dark matter annihilation signals; and "shake it" to dark matter scattering. This section discusses the current status of these detection methods.

1.3.1 Collider Bounds

If dark matter is produced in a collider, it will simply leave the detector without depositing any energy. To determine if such an invisible particle was produced, conservation of energy-momentum is used to determine if any events are missing energy. In practice, what is searched for is missing momentum that is transverse to the beamline.

Currently, dark matter has not been observed to be produced in particle colliders. This non-observation has instead been used to constrain the dark matter mass and production cross-sections or couplings of various models. These limits are typically interpreted in a model-dependent manner, as different dark matter - Standard model couplings can significantly alter the production rates.

The ATLAS and CMS experiments at the LHC have performed analyses on various dark matter production mechanisms, including the exchange of a Z/Z' or Higgs, EFTs and heavy mediators, and mono-jet searches [42][8]. Collider searches also offer complimentary probes of the dark matter-nucleon scattering cross-section [43] as they probe the same underlying coupling of dark matter to quarks.

It is important to note that an observation of an invisible massive particle at a collider is not enough to infer that it is dark matter. Such an observation will only tell us that such a particle exists. On its own, it does not determine the abundance of the species or if it is stable in cosmological times. As such, it could be just a sub-component of a larger dark sector. To measure enough of the model parameters and determine these important properties, complimentary observations from direct or indirect detectors are often required.

[8]These searches refer to a single jet being produced alongside a pair of dark matter particles. This jet could be of Standard Model or dark sector origin, with the latter commonly referred to as "mono-X" searches.

1.3.2 Direct Detection Searches

In colliders, dark matter with mass below the collision energy can be produced as long as it couples to the electroweak or colour sectors of the SM. Direct detection experiments, on the other hand, must employ different experimental techniques to probe different mass ranges. For ALP dark matter that is wavelike, haloscope experiments such as ADMX [44] and MADMAX [45] attempt to convert ALPs to photons via the Primakoff effect. Searches for WIMP-like dark matter look for the dark matter scattering with some detector material, causing it to recoil and deposit energy into the detector. Given that our focus is on WIMP-like dark matter, this section will review the status of these experiments.

The differential rate at which the incoming flux of dark matter will scatter within a detector with N_T targets, as a function of the recoil energy, E_R, is given by

$$\frac{dR(E_R,t)}{dE_R} = N_T \frac{\rho_{\rm DM}}{m_{\rm DM}} \int_{v>v_{\rm min}}^{v_{\rm esc}} v f(\vec{v}+\vec{v}_E) \frac{d\sigma}{dE_R}\, d^3v, \tag{1.24}$$

and depends on the quantities:

- $v_{\rm min}$ is the minimum dark matter velocity required by kinematics for a scattering event to occur;
- $v_{\rm esc} = 528\,{\rm km\,s^{-1}}$ is the Milky Way escape velocity;
- $\vec{v}_E$ is the velocity of the Earth through the dark matter halo[9];
- $f(\vec{v}-\vec{v}_E)$ is the dark matter velocity distribution in the Earth's frame;
- $d\sigma/dE_R$ is the differential scattering cross-section.

Given the low interaction rate of dark matter, the expected event rate in detectors is very low, around one event per day, per kilogram of target material, per kiloelectronvolt deposited. To contend with such a low event rate, as much of the background noise needs to be reduced as possible. This is achieved by placing the detectors deep underground in laboratories that are naturally shielded from the majority of the cosmic rays incident on the surface.

The particle physics input into the scattering rate is encapsulated within the differential cross-section, $d\sigma/dE_R$. It is common to separate the cross-section into contributions from spin-dependent (SD) and spin-independent (SI) interactions such

[9] This accounts for the orbit of the Earth around the Sun, which induces an annual modulation in the flux of DM.

that

$$\frac{d\sigma}{dE_R} = \frac{(m_{\rm DM}+m_{\rm T})^2}{m_T m_{\rm DM}^2 v^2}\left(\sigma^{\rm SI}|F_{\rm SI}(E_R)|^2 + \sigma^{\rm SD}|F_{\rm SD}(E_R)|^2\right), \tag{1.25}$$

$$\sigma^{\rm SI} \approx \sigma_0^{\rm SI} A_T^2 \left(\frac{m_T}{m_p}\right)^2 \left(\frac{m_{\rm DM}+m_p}{m_{\rm DM}+m_T}\right)^2, \tag{1.26}$$

$$\sigma^{\rm SD} \approx \sigma_0^{\rm SD} \left(\frac{4(J_T+1)}{3J_T}|\langle S_p\rangle + \langle S_n\rangle|^2\right)\left(\frac{m_T}{m_p}\right)^2 \left(\frac{m_{\rm DM}+m_p}{m_{\rm DM}+m_T}\right)^2, \tag{1.27}$$

where m_T, A_T, J_T are the target mass, atomic mass number, and atomic spin, m_p is the mass of the proton, $\langle S_{p,n}\rangle$ are the expectation values of the protons and neutrons in the nucleus. The $\sigma_{p,0}^{\rm SI/SD}$ are reference DM-proton scattering cross-sections evaluated in the zero-momentum transfer limit, with the form factors $F_{\rm SI/SD}(E_R)$ depending on the recoil energy accounting for the finite size of the nucleus being probed at high momentum transfer. We have assumed that dark matter interacts the same with neutrons and protons for simplicity.

The SI interactions do not couple to the spin of the target and as such the nuclear cross-section is a coherent sum over all the nucleons. This results in an A_T^2 enhancement compared to the dark matter-nucleon cross-section. Experiments searching for SI interactions take advantage of this by using heavy noble gases as the target material, such as Xenon and Argon. On the other hand, the SD interactions do couple to the spin of the target. As the total cross-section is the sum of all the nucleon contributions, the result is expected to average out to zero unless there is an unpaired nucleon present. Chemicals that contain ^{19}F are the favourable targets as it contains an unpaired proton.

The current leading constraints on the dark matter-nucleon scattering cross-section are shown in Fig. 1.5, with SI in the top panel and SD in the bottom. The SI limits are set by liquid noble gas experiments (LZ [46], XENON-1T [47], PandaX-II [48], and DarkSide-50 [49]), solid-state cryogenic detectors (CRESST-III [50], CDMSlite [51], with projected DARWIN sensitivities [52]), and room temperature crystals (DAMA/LIBRA [53], and COSINE-100 [54]).

The constraints on the SD dark matter-proton scattering cross-section are shown in the bottom panel of Fig 1.5. Superheated liquid experiments such as the PICO-60 [55] as well as PICASSO [56] provide the leading constraints. These interactions are also constrained by many of the same experiments taht focus on SI interactions, as they will inevitably contain isotopes with non-zero spin, such as ^{129}Xe and ^{131}Xe in XENONnT.

The orange dashed line represents the neutrino floor[10], providing a lower limit on the cross-section that can be probed by conventional direct detection experiments. Below this line, detectors will become sensitive to the irreducible background from

[10]Calling this the "neutrino fog" rather than floor has been gaining traction in recent years [57]

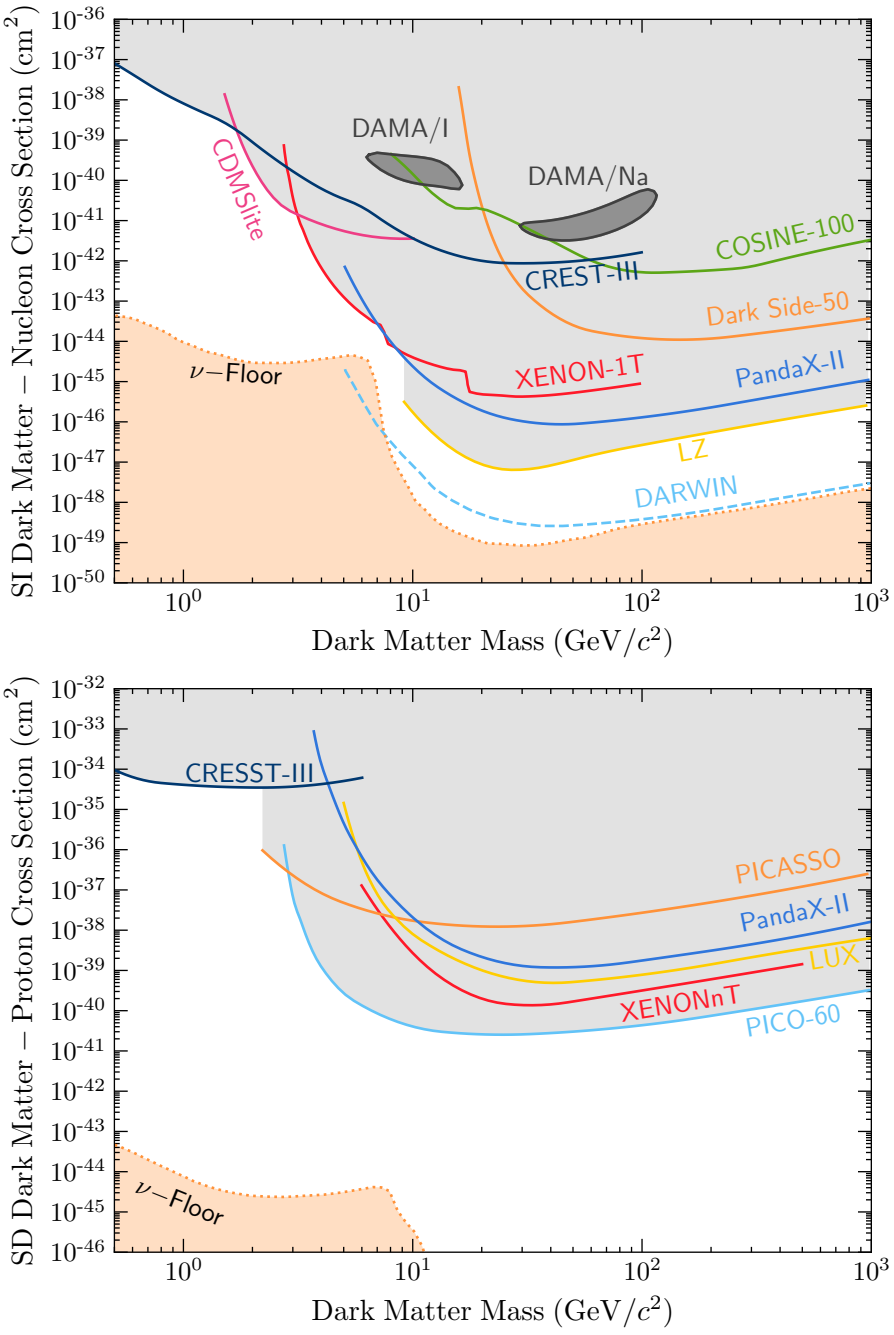

Figure 1.5: Current status of direct detection searches for dark matter. **Top:** Spin-independent dark matter-nucleon scattering. **Bottom:** Spin-dependent dark matter-proton scattering. Shaded regions above the coloured lines are excluded. Data was taken from the sources cited in the text.

Coherent Elastic Neutrino-Nucleus Scattering (CEνNS). For dark matter masses $\lesssim 10\,\text{GeV}$ the solar neutrino flux is the main background source, while the atmospheric neutrino flux becomes the dominant background for masses $\gtrsim 20\,\text{GeV}$. A significant amount of effort is being put toward overcoming this limitation, with the main strategy being to take advantage of the directionality of dark matter flux [58]. Such experiments attempt to resolve the direction of the nuclear recoil event, giving information about the direction the incident particle came from. This could allow discrimination between dark matter events, that are expected to be from the direction of the Cygnus constellation, and the background solar and atmospheric neutrinos coming from the Sun and sky respectively.

Many experiments begin to lose sensitivity to low-mass dark matter ($m_{\text{DM}} \lesssim 10\,\text{GeV}$) as the recoil energy of the targets falls below the threshold energy resolution of the detector. Current detectors can reach thresholds as low as $\sim \mathcal{O}(100\,\text{eV})$, which is on the same order of magnitude as the recoil energy due to a 1 GeV dark matter collision.

On the other hand, above $\sim 10\,\text{GeV}$ the sensitivities of the experiments all decrease at a rate inversely proportional to the dark matter mass. This is due to the interaction rate in Eq. 1.24 being proportional to the number of dark matter particles that pass through the detector, $N_{\text{DM}} = \rho_{\text{DM}}/m_{\text{DM}}$. As the local dark matter density is observed to be $\rho_{\text{DM}} = 0.4\,\text{GeV}\,\text{cm}^{-3}$, N_{DM} decreases as the dark matter mass increases, and hence so do the detector sensitivities.

Direct detection limits also assume that the scattering cross-section is independent of the dark matter velocity and momentum transfer in the interaction. Given that the local dark matter dispersion velocity is predicted to be $v_d = 270\,\text{km}\,\text{s}^{-1} \approx 10^{-3}c$, a back-of-the-envelope estimation for the momentum transfer gives $q_{\text{tr}} \lesssim 100\,\text{MeV}$. Therefore, cross-sections proportional to v_{DM} or q_{tr} will result in significantly lower event rates and hence much weaker limits than the unsuppressed interactions.

1.3.3 Indirect Detection

This leads us to indirect detection methods, which can provide complementary probes to direct detection while also exploring interactions that are difficult, if not impossible, for terrestrial-based detectors to observe. Indirect detection experiments aim to infer the presence of dark matter through its annihilation or decay into Standard Model states. These searches look for dark matter annihilation products from astrophysical sources, including:

- Gamma-rays at terrestrial-based telescopes such as HESS [59–61], VERITAS [62–64], MAGIC [65, 66] and HAWC [67–70] as well as the Fermi-LAT [71–75] satellite;

- Neutrino signals at IceCube [76, 77], ANTARES [78–80], Super-K [81–83], and will be searched for at the upcoming Hyper-K [84–86], JUNO [87] experiments.

- Cosmic-Ray antimatter excess observed by the AMS-02 experiment [88, 89]

Signals from dark matter annihilation are best searched for by looking at regions where the dark matter density is expected to be high, boosting the annihilation rate. Natural places to look include the Galactic Centre [90, 91], dwarf-spheroidal galaxies [92], and celestial bodies where dark matter can accumulate over time. The latter scenario is central to this work and was pioneered by considering the effects of dark matter being captured within the Sun.

1.4 Dark Matter Signals from the Sun

Stars have a rich history of being used as astrophysical laboratories to help in the search for dark matter. Depending on the type of dark matter being searched for, there are various signals one can look for. Light bosonic dark matter, such as ALPs and dark photons, can be produced within the plasma of stars, altering the energy transport properties within them. This can ultimately lead to deviations in the evolution of the star, which can be used to place some of the strongest constraints on these models [93–95]. WIMP-like dark matter in the halo that couples to visible matter can scatter within the stars as they pass through. If the dark matter loses enough energy in these interactions, it can become gravitationally bound to the object and a population of dark matter will be accumulated within the star over time [23, 96–99].

This idea of WIMPs accumulating within the cores of stars has been applied extensively to the star closest to us, the Sun. The formalism for stellar capture of dark matter was set up by Gould [97, 98, 100] in the late 80's, and has remained quite successful to this day, with many authors continuing to build upon these foundations over time [99, 101, 102].

Once the dark matter is captured, it will continue to scatter with the stellar constituents until it thermalises within the core of the Sun, collecting with an isothermal sphere. The radius of this sphere can be found by applying the virial theorem, with the gravitational potential given by

$$\Phi(r) = -\int_r^\infty \frac{GM_\odot(r')}{r'^2} dt', \tag{1.28}$$

$$\approx \frac{2}{3}\pi G \rho_{\odot,c} r^2, \tag{1.29}$$

assuming the density of the Sun within this region is constant, $\rho_{\odot,c}$. The resulting radius is

$$r_{\rm iso}^2 = \frac{3T_\odot}{2\pi G m_{\rm DM}\rho_\odot}. \tag{1.30}$$

The dark matter number density will follow a Gaussian profile,

$$n_{\rm iso}(r) = n_0 \exp\left(-\frac{m_{\rm DM}\Phi(r)}{T_\odot}\right), \tag{1.31}$$

$$= n_0 \exp(-r^2/r_{\rm iso}^2), \tag{1.32}$$

where n_0 is a normalistion constant fixed by requiring that the total number of dark matter particles is

$$N_{\rm DM} = \int d^3r\, n_{\rm iso}(r). \tag{1.33}$$

In addition, dark matter velocity will follow a Maxwell-Boltzmann distribution,

$$f_{\rm MB}(v) = 4\pi\left(\frac{m_{\rm DM}}{4\pi T_\odot}\right)^{3/2} v^2 \exp\left[-\frac{m_{\rm DM}v^2}{4T_\odot}\right]. \tag{1.34}$$

The time evolution of the total number of dark matter particles within the Sun is governed by three processes. Capture acts to increase the number over time, while annihilation and evaporation will reduce this number over time. This is described by the differential equation

$$\frac{dN_{\rm DM}}{dt} = C - EN_{\rm DM} - AN_{\rm DM}^2, \tag{1.35}$$

where C and E are the capture and evaporation rates respectively, with A being related to the annihilation rate, $\Gamma_{\rm ann}$ through

$$\Gamma_{\rm ann} = \frac{1}{2}\int dr^3 n_{\rm iso}^2(r)\langle\sigma_{\rm ann}v\rangle \tag{1.36}$$

$$\equiv \frac{1}{2}AN_{\rm DM}^2, \tag{1.37}$$

where the factor of 1/2 accounts for each annihilation removing two dark matter particles from the Sun.

In this context, evaporation refers to the process in which dark matter can be ejected back out of the Sun by up-scattering[11] off an energetic constituent. This

[11] Up-scattering refers to the interactions in which the dark matter gains rather than loses energy.

becomes increasingly important for lighter dark matter masses, as less energy will be required to boost the dark matter above the local escape velocity. Below a certain mass, the capture and evaporation come into equilibrium, and a net-zero amount of dark matter is contained within the Sun. This critical mass places a lower bound on the dark matter mass that can be probed through stellar capture and is named the evaporation mass, m_{evap}.

There are three regimes we are interested in solving this equation for. The simplest case is when evaporation and annihilation are both negligible, then the solution is simply,

$$N_{\text{DM}}(t) = Ct, \tag{1.38}$$

indicating that the dark matter will simply continue to grow over time.

Next, assume that annihilations are negligible ($A = 0$), while capture and evaporation are present. The result is

$$N_{\text{DM}}(t) = Ct\left(\frac{1 - e^{-Et}}{Et}\right), \tag{1.39}$$

where the first factor is the number of captured dark matter if evaporation is negligible. From this, we can estimate the evaporation mass by asking when the evaporation rate is large enough to cause a significant reduction in the number of captured dark matter particles relative to the $E = 0$ case. This can be expressed formally as [101]

$$\frac{1}{N_{\text{DM}}(m_{\text{evap}})}\left|N_{\text{DM}}(m_{\text{evap}}) - \frac{C(m_{\text{evap}})}{E(m_{\text{evap}})}\right| = \alpha, \tag{1.40}$$

where α is the fraction of evaporated dark matter, taken to be $\sim 10\%$.

Finally, consider the case in which evaporation can be neglected, $m_{\text{DM}} \gtrsim m_{\text{evap}}$. The solution in this regime is

$$N_{\text{DM}}(t) = \sqrt{\frac{C}{A}}\tanh(\sqrt{CA}t) \overset{t\to\infty}{\longrightarrow} \sqrt{\frac{C}{A}}, \tag{1.41}$$

that reaches an equilibrium state between capture and annihilation for times longer than the characteristic scale, $t_{\text{eq}} = 1/\sqrt{CA}$. This state is known as capture-annihilation equilibrium.

The signals searched for depend on whether the dark matter can annihilate or not. If the dark matter is asymmetric, it cannot annihilate, and we can set $A = 0$ in Eq. 1.35. This leads to the population continuing to grow over time, with $N_{\text{DM}}(t) = Ct$ if evporation is negligible. A large enough population of captured dark matter can alter the energy transport within the Sun, leading to the modifications of the solar neutrino flux, or even the solar structure itself [87, 103–105].

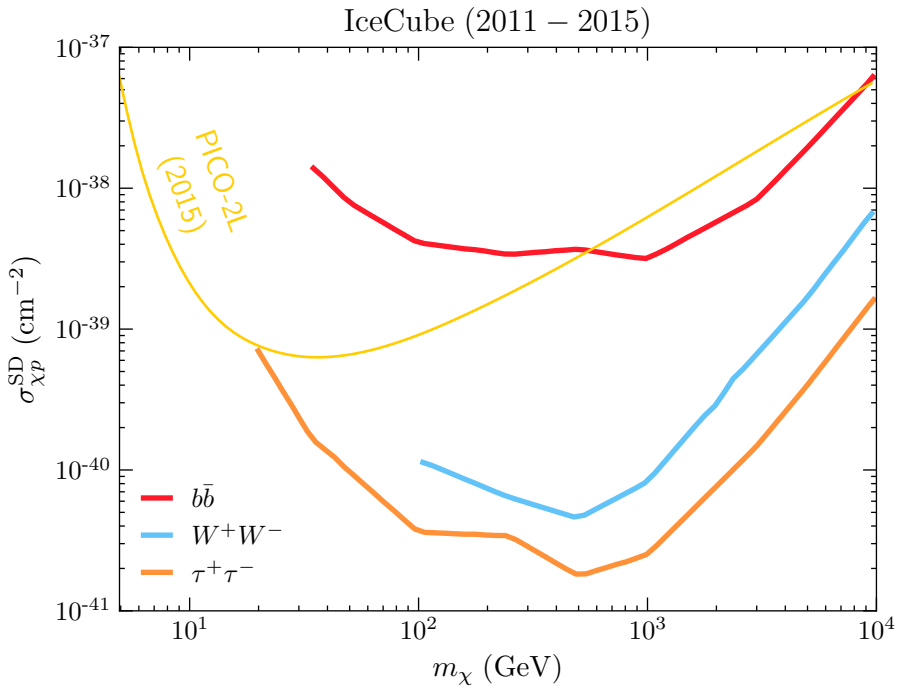

Figure 1.6: Limits on the SD dark matter-proton cross-section from the IceCube collaboration assuming 100% branching fraction to $b\bar{b}$ (red), W^+W^- (blue) or $\tau^+\tau^-$ (orange) final states. Also shown is the result from the PICO-2L DD experiment. This plot was recreated with data taken from Ref. [76].

Instead, if the dark matter can annihilate an equilibrium will eventually be reached between the capture and annihilation rates, and the total number of dark matter particles will be constant. If the annihilation products can escape the Sun, they can be searched for by various experiments depending on the nature of the final states. These could be neutrinos produced from the decays of other charged annihilation products [79–81, 106, 107], or to some other long-lived state that can escape the Sun and decay into visible states [108–112].

In comparison to DD searches, interpretation of indirect detection data will require additional model-dependent assumptions, namely the relevant annihilation channels of the dark matter. The most general limits can be placed by assuming that the dark matter only has a single annihilation channel, i.e. annihilation to a $\tau^+\tau^-$ final state 100% of the time. Under these assumptions, limits on the SD dark matter-proton cross-section have been placed that exceed current DD constraints, due to the rather large abundance of Hydrogen within the Sun. Constraints from the IceCube collaboration are shown in Fig. 1.6

Change

Overcoming the first issue requires either a colder star or one that is much

heavier. The second requires dark matter to scatter with the constituent material at relativistic energies to overcome the suppression in the cross-sections. Fortunately, there exist objects that meet all these criteria, allowing for a wider variety of dark matter models to be explored than direct detection or traditional indirect detection experiments: compact objects.

1.5 Compact Objects as Dark Matter Probes

The main goal behind this work is to explore how compact objects can be used to probe a wide variety of dark matter interactions that terrestrial direct detection experiments are insensitive to. By compact objects, we are referring to Neutron Stars (NSs) and White Dwarfs (WDs), and not Black Holes that also fall into this category.

Compact objects offer a unique laboratory for studying dark matter and its interactions with the Standard Model in environments unachievable anywhere else in the Universe. They generate strong gravitational fields and are composed of incredibly dense matter, with NSs reaching super-nuclear densities in their central cores. The capture rate within these objects is therefore enhanced due to these properties, with benefits over solar capture including:

- **Gravitational focusing of the DM flux:** The strong gravitational field will increase the impact parameter of the infalling dark matter. This increases the effective size of the capturing body, increasing the flux of dark matter passing through it.

- **Realtivistic Interaction Energies:** In general, the infalling dark matter will be accelerated to (semi-)relativistic velocities ($\sim 0.2 - 0.7c$). Moreover, the stellar constituents will also have relativistic energies. As such, interactions that are momentum/velocity dependent will suffer far less suppression than in DD experiments.

- **Large Number of Targets:** The extremely high densities of these objects correspond to a considerable number of targets for scattering to occur. This allows these objects to probe very small scattering cross-sections, with NSs in particular expected to reach as low as $\sim 10^{-45}\,\mathrm{cm}^2$.

- **Low Evpaortion Masses**: Relative to the Sun, the evaporation mass in compact objects can be quite low, on the order of keV in some cases. This is due to in part to the increased gravitational strength, but main to the significantly lower temperatures in old compact objects.

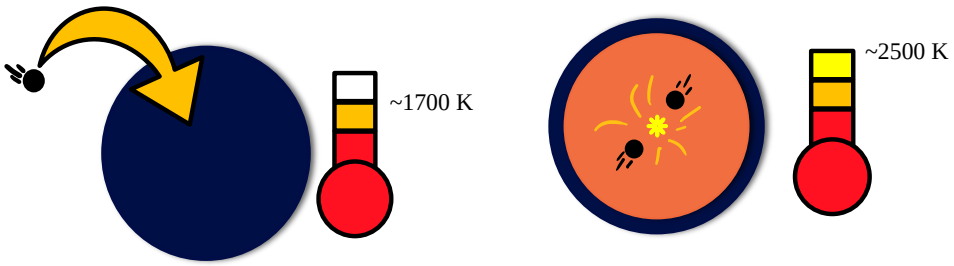

Figure 1.7: Illustration of DM-induced heating of compact objects. **Left:** kinetic heating due to DM scattering, raising the temperature to $\sim 1700\,\mathrm{K}$. **Right:** Annihilation heating contributes an additional $\sim 800\,\mathrm{K}$. This image is inspired by Ref. [130].

In the past, capture in NSs has been applied primarily in the context of sending gravitational collapse into black holes [113–119], and the modifications of NS merger rates as well as the gravitational wave signatures of these mergers [120–123]. Capture in WDs has also been considered, with a variety of different applications of the capture process [124–129].

In recent years, dark matter induced heating of NSs has reemerged as a potential detection frontier [130–137]. It was shown that dark matter could reheat old, isolated NSs in our local neighbourhood[12] back up to temperatures that would cause them to radiate as blackbody peaked in the near-infrared. The aim is to locate the NSs with radio telescopes such as the Square-Kilometer-Array (SKA), and determine their age through their spindown rate. Once located, the star's temperature can be determined through observations from infrared telescopes such as the James Webb Space Telescope (JWST).

This heating occurs in two stages. The dark matter will first deposit its kinetic energy into the star through the scatterings required for capture and its subsequent thermalisation within the NS core, with this process called *kinetic heating*. If the dark matter can annihilate, it will deposit its mass energy, assuming the products are trapped within the star, termed *annihilation heating*. These processes are illustrated in Fig. 1.7. Assuimng a NS in our local neighbourhood

In order to accurately determine the limits on dark matter interactions that such an observation could place, one first requires an accurate calculation of the capture rate. However, all previous calculations relied on the formalism set up by Gould for capture in the Sun, with only minor modifications made to accommodate the extreme nature of the compact objects.

[12]Local neighbourhood refers to the region within $\sim 1\,\mathrm{kpc}$ of the Sun.

1.6 Thesis Outline

Chapters **??** and **??** of this thesis are devoted to reformulating Gould's capture formalism to account for the physics specific to compact objects in a self-consistent manner. These include a relativistic treatment of the kinematics, using General Relativity to calculate the correct dark matter flux passing through the star, and accounting for Pauli blocking of the final state target using Fermi-Dirac statistics for the stellar constituents. In addition, we incorporate the internal structure of these objects by calculating the radial profiles for the relevant microscopic quantities (e.g., chemical potentials and number densities) via the adoption of a realistic equation of state.

Further considerations are required when considering dark matter interactions with the baryonic matter inside NSs. Due to the high density of the NS interior, the baryonic matter undergoes strong interactions amongst themselves and should not be treated as a free Fermi gas. Instead, adopting an equation of state that accounts for these interactions is required. These interactions modify the mass of the baryons, leading them to obtain an effective mass smaller than their vacuum mass. Furthermore, as we will see, the dark matter may interact with the baryons with momentum transfers on the order of 10 GeV. This is high enough that the dark matter will begin to resolve the internal structure of the baryon. To account for this, the momentum dependence of the baryon form factors that are typically neglected in direct detection and solar capture must be reintroduced.

This formalism is made in preparation for a thorough analysis of the timescales involved in the dark matter heating of compact objects. The enrgy deposited in both the kinetic and annihilation heating stages does not occur instantaneously, and the timescales involved in them need to be compared to the age of the star in question. We will define kinetic heating timescale as the time required for dark matter to deposit 99% of its initial kinetic energy into the star. For annihilation heating to occur, the dark matter must reach a state of capture-annihilation equilibrium within the stellar core. In standard calculations of this timescale, the dark matter must first become thermalised with the star. Only then can annihilations occur efficiently enough to heat the star.

We will work with the EFT operators in Table 1.1 that describe Dirac fermion dark matter interacting with Standard Model leptons. Each operator will be studied in isolation, i.e., by considering a Lagrangian that contains only one of the operators rather than a linear superposition of multiple. This way, we can analyse specific types of interactions independently, allowing us to take as model-independent an approach to the phenomenology as possible.

Definition of Symbols and Abbreviations

ALP Axion Like Particle

BBN Big Bang Nucleosynthesis

$\boldsymbol{C_{\text{geo}}}$ Geometric Capture Rate
CMB Cosmic Microwave Background

DD Direct Detection
DM Dark Matter
$\boldsymbol{K_\chi}$ Dark Matter Kinetic Energy
$\boldsymbol{\rho_\chi}$ DM halo density
$\boldsymbol{m_\chi}$ Dark Matter Mass

EFT Effective Field Theory
EoS Equation of State

$\boldsymbol{f_{\text{FD}}}$ Fermi-Dirac Distribution
$\boldsymbol{\varepsilon_{F,i}}$ Fermi kinetic energy of target species

JWST James Webb Space Telescope

$\boldsymbol{|\overline{\mathcal{M}}|^2}$ Spin-averaged squared matrix element
$\boldsymbol{\mu}$ DM-Target mass ratio, m_χ/m_i

nEMD Neutron ELectric Dipole Moment
NS Neutron Star

PB Pauli Blocking
PQ Peccei-Quinn

QMC Quark-Meson-Coupling EoS

$\boldsymbol{\sigma_{\text{th}}}$ Threshold Cross-Section
SM Standard Model

$\boldsymbol{T_{\text{eq}}}$ Equilibrium Temperature
$\boldsymbol{t_{\text{eq}}}$ Capture-Annihilation equilibrium time
$\boldsymbol{T_\star}$ Temperature of the star
$\boldsymbol{t_{\text{therm}}}$ Thermalisation time

UV Ultraviolet

$\boldsymbol{v_d}$ DM halo dispersion velocity
$\boldsymbol{v_\star}$ Star velocity

WD White Dwarf
WIMP Weakly Interacting Massive Particle

Bibliography

[1] F. Zwicky. "On the Masses of Nebulae and of Clusters of Nebulae". In: *The Astrophysical Journal* 86 (1937), pp. 217–246. DOI: 10.1086/143864.

[2] Julio F. Navarro, Carlos S. Frenk, and Simon D. M. White. "The Structure of Cold Dark Matter Halos". In: *The Astrophysical Journal* 462 (1996), pp. 563–575. DOI: 10.1086/177173. arXiv: astro-ph/9508025.

[3] Julio F. Navarro, Carlos S. Frenk, and Simon D. M. White. "A Universal Density Profile from Hierarchical Clustering". In: *The Astrophysical Journal* 490.2 (1997), pp. 493–508. DOI: 10.1086/304888. arXiv: astro-ph/9611107.

[4] J. Einasto. "On the Construction of a Composite Model for the Galaxy and on the Determination of the System of Galactic Parameters". In: *Trudy Astrofizicheskogo Instituta Alma-Ata* 5 (Jan. 1, 1965), pp. 87–100.

[5] Katherine Freese. "Review of Observational Evidence for Dark Matter in the Universe and in Upcoming Searches for Dark Stars". In: *EAS Publications Series* 36 (May 30, 2009), pp. 113–126. DOI: 10.1051/eas/0936016. arXiv: 0812.4005 [astro-ph].

[6] Federico Lelli, Stacy S. McGaugh, and James M. Schombert. "SPARC: Mass Models for 175 Disk Galaxies with Spitzer Photometry and Accurate Rotation Curves". In: *The Astronomical Journal* 152.6 (2016), p. 157. DOI: 10.3847/0004-6256/152/6/157. arXiv: 1606.09251 [astro-ph.GA].

[7] Peter Schneider, Christopher S. Kochanek, and Joachim Wambsganss. *Gravitational Lensing: Strong, Weak and Micro*. In collab. with Saas-fee advanced course. Berlin New York: Springer, 2006.

[8] J. K. Adelman-McCarthy et al. "The Fourth Data Release of the Sloan Digital Sky Survey". In: *The Astrophysical Journal Supplement Series* 162.1 (2006), pp. 38–48. DOI: 10.1086/497917. arXiv: astro-ph/0507711.

[9] Rachel Mandelbaum et al. “Galaxy Halo Masses and Satellite Fractions from Galaxy-Galaxy Lensing in the Sdss: Stellar Mass, Luminosity, Morphology, and Environment Dependencies”. In: *Mon. Not. Roy. Astron. Soc.* 368 (2006), p. 715. DOI: 10.1111/j.1365-2966.2006.10156.x. arXiv: astro-ph/0511164.

[10] Douglas Clowe, Anthony Gonzalez, and Maxim Markevitch. “Weak Lensing Mass Reconstruction of the Interacting Cluster 1E0657-558: Direct Evidence for the Existence of Dark Matter”. In: *The Astrophysical Journal* 604.2 (2004), pp. 596–603. DOI: 10.1086/381970. arXiv: astro-ph/0312273.

[11] Scott W. Randall et al. “Constraints on the Self-Interaction Cross-Section of Dark Matter from Numerical Simulations of the Merging Galaxy Cluster 1E 0657-5”. In: *The Astrophysical Journal* 679.2 (2008), pp. 1173–1180. DOI: 10.1086/587859. arXiv: 0704.0261 [astro-ph].

[12] N. Aghanim, Y. Akrami, M. Ashdown, et al. “Planck 2018 Results. VI. Cosmological Parameters”. In: *Astronomy & Astrophysics* 641 (Sept. 1, 2020), A6. DOI: 10.1051/0004-6361/201833910. arXiv: 1807.06209 [astro-ph.CO].

[13] N. Aghanim, Y. Akrami, M. Ashdown, et al. “Planck 2018 Results. V. CMB Power Spectra and Likelihoods”. In: *Astronomy & Astrophysics* 641 (Sept. 1, 2020), A5. DOI: 10.1051/0004-6361/201936386. arXiv: 1907.12875 [astro-ph.CO].

[14] Volker Springel, Carlos S. Frenk, and Simon D. M. White. “The Large-Scale Structure of the Universe”. In: *Nature* 440.7088 (2006), p. 1137. DOI: 10.1038/nature04805. arXiv: astro-ph/0604561.

[15] Volker Springel et al. “Simulating the Joint Evolution of Quasars, Galaxies and Their Large-Scale Distribution”. In: *Nature* 435.7042 (2005), pp. 629–636. DOI: 10.1038/nature03597. arXiv: astro-ph/0504097.

[16] Samuel D. McDermott, Hai-Bo Yu, and Kathryn M. Zurek. “Turning off the Lights: How Dark Is Dark Matter?” In: *Physical Review D* 83.6 (2011), p. 063509. DOI: 10.1103/PhysRevD.83.063509. arXiv: 1011.2907 [hep-ph].

[17] Sean Tulin and Hai-Bo Yu. “Dark Matter Self-interactions and Small Scale Structure”. In: *Physics Reports* 730 (Feb. 5, 2018), pp. 1–57. DOI: 10.1016/j.physrep.2017.11.004. arXiv: 1705.02358 [hep-ph].

[18] David N. Spergel and Paul J. Steinhardt. “Observational Evidence for Self-Interacting Cold Dark Matter”. In: *Physical Review Letters* 84.17 (2000), pp. 3760–3763. DOI: 10.1103/PhysRevLett.84.3760. arXiv: astro-ph/9909386.

[19] David A. Buote et al. “Chandra Evidence for a Flattened, Triaxial Dark Matter Halo in the Elliptical Galaxy NGC 720”. In: *The Astrophysical Journal* 577.1 (2002), pp. 183–196. DOI: 10.1086/342158. arXiv: astro-ph/0205469.

[20] R. L. Workman et al. “Review of Particle Physics”. In: *PTEP* 2022 (Aug. 8, 2022), p. 083C01. DOI: 10.1093/ptep/ptac097.

[21] H. Goldberg. “Constraint on the Photino Mass from Cosmology”. In: *Phys. Rev. Lett.* 50 (1983). Ed. by M. A. Srednicki, p. 1419. DOI: 10.1103/PhysRevLett.50.1419.

[22] Edward W. Kolb and Richard Slansky. “Dimensional Reduction in the Early Universe: Where Have the Massive Particles Gone?” In: *Phys. Lett. B* 135 (1984), p. 378. DOI: 10.1016/0370-2693(84)90298-3.

[23] Gerard Jungman, Marc Kamionkowski, and Kim Griest. “Supersymmetric Dark Matter”. In: *Phys. Rept.* 267 (1996), pp. 195–373. DOI: 10.1016/0370-1573(95)00058-5. arXiv: hep-ph/9506380.

[24] Gary Steigman, Basudeb Dasgupta, and John F. Beacom. “Precise Relic WIMP Abundance and Its Impact on Searches for Dark Matter Annihilation”. In: *Phys. Rev. D* 86 (2012), p. 023506. DOI: 10.1103/PhysRevD.86.023506. arXiv: 1204.3622 [hep-ph].

[25] Tsung-Han Yeh et al. “Probing Physics beyond the Standard Model: Limits from BBN and the CMB Independently and Combined”. In: *JCAP* 10 (Oct. 14, 2022), p. 046. DOI: 10.1088/1475-7516/2022/10/046. arXiv: 2207.13133 [astro-ph.CO].

[26] Kim Griest and Marc Kamionkowski. “Unitarity Limits on the Mass and Radius of Dark Matter Particles”. In: *Phys. Rev. Lett.* 64 (1990), p. 615. DOI: 10.1103/PhysRevLett.64.615.

[27] C. Abel et al. “Measurement of the Permanent Electric Dipole Moment of the Neutron”. In: *Phys. Rev. Lett.* 124.8 (Feb. 29, 2020), p. 081803. DOI: 10.1103/PhysRevLett.124.081803. arXiv: 2001.11966 [hep-ex].

[28] Frank Wilczek. “Problem of Strong P and T Invariance in the Presence of Instantons”. In: *Phys. Rev. Lett.* 40 (1978), pp. 279–282. DOI: 10.1103/PhysRevLett.40.279.

[29] Steven Weinberg. “A New Light Boson?” In: *Phys. Rev. Lett.* 40 (1978), pp. 223–226. DOI: 10.1103/PhysRevLett.40.223.

[30] Jihn E. Kim. “Weak Interaction Singlet and Strong CP Invariance”. In: *Phys. Rev. Lett.* 43 (1979), p. 103. DOI: 10.1103/PhysRevLett.43.103.

[31] Mikhail A. Shifman, A. I. Vainshtein, and Valentin I. Zakharov. "Can Confinement Ensure Natural CP Invariance of Strong Interactions?" In: *Nucl. Phys. B* 166 (1980), pp. 493–506. DOI: 10.1016/0550-3213(80)90209-6.

[32] A. R. Zhitnitsky. "On Possible Suppression of the Axion Hadron Interactions. (In Russian)". In: *Sov. J. Nucl. Phys.* 31 (1980), p. 260.

[33] Michael Dine, Willy Fischler, and Mark Srednicki. "A Simple Solution to the Strong CP Problem with a Harmless Axion". In: *Phys. Lett. B* 104 (1981), pp. 199–202. DOI: 10.1016/0370-2693(81)90590-6.

[34] Stephen Hawking. "Gravitationally Collapsed Objects of Very Low Mass". In: *Mon. Not. Roy. Astron. Soc.* 152 (Apr. 1, 1971), p. 75. DOI: 10.1093/mnras/152.1.75.

[35] B. J. Carr and S. W. Hawking. "Black Holes in the Early Universe". In: *Monthly Notices of the Royal Astronomical Society* 168 (1974), pp. 399–415. DOI: 10.1093/mnras/168.2.399.

[36] B. J. Carr. "The Primordial Black Hole Mass Spectrum." In: *The Astrophysical Journal* 201 (1975), pp. 1–19. DOI: 10.1086/153853.

[37] Paulo Montero-Camacho et al. "Revisiting Constraints on Asteroid-Mass Primordial Black Holes as Dark Matter Candidates". In: *Journal of Cosmology and Astroparticle Physics* 08.08 (Aug. 23, 2019), p. 031. DOI: 10.1088/1475-7516/2019/08/031. arXiv: 1906.05950 [astro-ph.CO].

[38] Pablo Villanueva-Domingo, Olga Mena, and Sergio Palomares-Ruiz. "A Brief Review on Primordial Black Holes as Dark Matter". In: *Frontiers in Astronomy and Space Sciences* 8 (May 11, 2021), p. 87. DOI: 10.3389/fspas.2021.681084. arXiv: 2103.12087 [astro-ph.CO].

[39] Jessica Goodman et al. "Constraints on Dark Matter from Colliders". In: *Physical Review D* 82.11 (2010), p. 116010. DOI: 10.1103/PhysRevD.82.116010. arXiv: 1008.1783 [hep-ph].

[40] Eugenio Del Nobile, Marco Cirelli, and Paolo Panci. "Tools for Model-Independent Bounds in Direct Dark Matter Searches". In: *Journal of Cosmology and Astroparticle Physics* 10.10 (Oct. 10, 2013), p. 019. DOI: 10.1088/1475-7516/2013/10/019. arXiv: 1307.5955 [hep-ph].

[41] "Electromagnetic Structure of the Nucleon". In: *The Structure of the Nucleon*. John Wiley & Sons, Ltd, 2001, pp. 7–51. DOI: 10.1002/352760314X.ch2.

[42] Albert M Sirunyan, Armen Tumasyan, Wolfgang Adam, et al. "Search for Dark Matter Produced with an Energetic Jet or a Hadronically Decaying W or Z Boson at Sqrt(s) = 13 TeV". In: *Journal of High Energy Physics* 07.7 (July 5, 2017), p. 014. DOI: 10.1007/JHEP07(2017)014. arXiv: 1703.01651 [hep-ex].

[43] F. Ruppin et al. "Complementarity of Dark Matter Detectors in Light of the Neutrino Background". In: *Physical Review D* 90.8 (Oct. 7, 2014), p. 083510. DOI: 10.1103/PhysRevD.90.083510. arXiv: 1408.3581 [hep-ph].

[44] S. J. Asztalos et al. "A SQUID-based Microwave Cavity Search for Dark-Matter Axions". In: *Phys. Rev. Lett.* 104 (2010), p. 041301. DOI: 10.1103/PhysRevLett.104.041301. arXiv: 0910.5914 [astro-ph.CO].

[45] P. Brun, A. Caldwell, L. Chevalier, et al. "A New Experimental Approach to Probe QCD Axion Dark Matter in the Mass Range above 40μeV". In: *The European Physical Journal C* 79.3 (Mar. 1, 2019), p. 186. DOI: 10.1140/epjc/s10052-019-6683-x. arXiv: 1901.07401 [physics.ins-det].

[46] J. Aalbers et al. "First Dark Matter Search Results from the LUX-ZEPLIN (LZ) Experiment". In: *Physical Review Letters* 131.4 (July 28, 2023), p. 041002. DOI: 10.1103/PhysRevLett.131.041002. arXiv: 2207.03764 [hep-ex].

[47] E. Aprile et al. "Search for Coherent Elastic Scattering of Solar ^{8}B Neutrinos in the XENON1T Dark Matter Experiment". In: *Phys. Rev. Lett.* 126 (Mar. 1, 2021), p. 091301. DOI: 10.1103/PhysRevLett.126.091301. arXiv: 2012.02846 [hep-ex].

[48] Yue Meng et al. "Dark Matter Search Results from the PandaX-4T Commissioning Run". In: *Phys. Rev. Lett.* 127.26 (Dec. 23, 2021), p. 261802. DOI: 10.1103/PhysRevLett.127.261802. arXiv: 2107.13438 [hep-ex].

[49] P. Agnes et al. "Search for Dark-Matter–Nucleon Interactions via Migdal Effect with DarkSide-50". In: *Phys. Rev. Lett.* 130.10 (Mar. 6, 2023), p. 101001. DOI: 10.1103/PhysRevLett.130.101001. arXiv: 2207.11967 [hep-ex].

[50] A.H. Abdelhameed, G. Angloher, P. Bauer, et al. "First Results from the CRESST-III Low-Mass Dark Matter Program". In: *Physical Review D* 100.10 (Nov. 26, 2019), p. 102002. DOI: 10.1103/PhysRevD.100.102002. arXiv: 1904.00498 [astro-ph.CO].

[51] M. F. Albakry et al. "A Search for Low-mass Dark Matter via Bremsstrahlung Radiation and the Migdal Effect in SuperCDMS". In: *Physical Review D* 107.11 (June 1, 2023), p. 112013. DOI: 10.1103/PhysRevD.107.112013. arXiv: 2302.09115 [hep-ex].

[52] J. Aalbers et al. "A Next-Generation Liquid Xenon Observatory for Dark Matter and Neutrino Physics". In: *J. Phys. G* 50.1 (Dec. 15, 2022), p. 013001. DOI: 10.1088/1361-6471/ac841a. arXiv: 2203.02309 [physics.ins-det].

[53] Christopher Savage et al. "Compatibility of DAMA/LIBRA Dark Matter Detection with Other Searches". In: *Journal of Cosmology and Astroparticle Physics* 04.04 (2009), p. 010. DOI: 10.1088/1475-7516/2009/04/010. arXiv: 0808.3607 [astro-ph].

[54] G. Adhikari et al. "Strong Constraints from COSINE-100 on the DAMA Dark Matter Results Using the Same Sodium Iodide Target". In: *Science Advances* 7.46 (Nov. 2021), abk2699. DOI: 10.1126/sciadv.abk2699. arXiv: 2104.03537 [hep-ex].

[55] C. Amole, M. Ardid, I.J. Arnquist, et al. "Dark Matter Search Results from the Complete Exposure of the PICO-60 C_3F_8 Bubble Chamber". In: *Physical Review D* 100.2 (July 10, 2019), p. 022001. DOI: 10.1103/PhysRevD.100.022001. arXiv: 1902.04031 [astro-ph.CO].

[56] E. Behnke et al. "Final Results of the PICASSO Dark Matter Search Experiment". In: *Astroparticle Physics* 90 (Apr. 2017), pp. 85–92. DOI: 10.1016/j.astropartphys.2017.02.005. arXiv: 1611.01499 [hep-ex].

[57] Ciaran A. J. O'Hare. "Fog on the Horizon: A New Definition of the Neutrino Floor for Direct Dark Matter Searches". In: *Physical Review Letters* 127.25 (Dec. 16, 2021), p. 251802. DOI: 10.1103/PhysRevLett.127.251802. arXiv: 2109.03116 [hep-ph].

[58] Philipp Grothaus, Malcolm Fairbairn, and Jocelyn Monroe. *Directional Dark Matter Detection Beyond the Neutrino Bound*. arXiv.org. June 19, 2014. DOI: 10.1103/PhysRevD.90.055018.

[59] H. Abdallah et al. "Search for γ-Ray Line Signals from Dark Matter Annihilations in the Inner Galactic Halo from 10 Years of Observations with H.E.S.S." In: *Phys. Rev. Lett.* 120.20 (May 16, 2018), p. 201101. DOI: 10.1103/PhysRevLett.120.201101. arXiv: 1805.05741 [astro-ph.HE].

[60] Alessandro Montanari and Emmanuel Moulin. "Search for Dark Matter Gamma-Ray Line Annihilation Signals in the H.E.S.S. Inner Galaxy Survey". In: *PoS* ICRC2023 (July 25, 2023), p. 1424. DOI: 10.22323/1.444.1424.

[61] F. Aharonian et al. "H.E.S.S. Observations of the Galactic Center Region and Their Possible Dark Matter Interpretation". In: *Phys. Rev. Lett.* 97 (2006), p. 221102. DOI: 10.1103/PhysRevLett.97.221102. arXiv: astro-ph/0610509.

[62] S. Archambault et al. “Dark Matter Constraints from a Joint Analysis of Dwarf Spheroidal Galaxy Observations with VERITAS”. In: *Phys. Rev. D* 95.8 (Apr. 5, 2017), p. 082001. DOI: 10.1103/PhysRevD.95.082001. arXiv: 1703.04937 [astro-ph.HE].

[63] James L. Ryan. “Search for Dark Matter Annihilation Signals in the Galactic Center Halo with VERITAS”. In: *PoS* ICRC2023 (July 25, 2023), p. 794. DOI: 10.22323/1.444.0794. arXiv: 2309.12403 [astro-ph.HE].

[64] Conor McGrath. “An Indirect Search for Dark Matter with a Combined Analysis of Dwarf Spheroidal Galaxies from VERITAS”. In: *PoS* ICRC2023 (July 25, 2023), p. 1395. DOI: 10.22323/1.444.1395.

[65] J. Aleksic et al. “MAGIC Gamma-Ray Telescope Observation of the Perseus Cluster of Galaxies: Implications for Cosmic Rays, Dark Matter and NGC 1275”. In: *Astrophys. J.* 710 (2010), pp. 634–647. DOI: 10.1088/0004-637X/710/1/634. arXiv: 0909.3267 [astro-ph.HE].

[66] J. Aleksic et al. “Searches for Dark Matter Annihilation Signatures in the Segue 1 Satellite Galaxy with the MAGIC-I Telescope”. In: *JCAP* 06 (2011), p. 035. DOI: 10.1088/1475-7516/2011/06/035. arXiv: 1103.0477 [astro-ph.HE].

[67] A. Albert et al. “Dark Matter Limits From Dwarf Spheroidal Galaxies with The HAWC Gamma-Ray Observatory”. In: *Astrophys. J.* 853.2 (Feb. 1, 2018), p. 154. DOI: 10.3847/1538-4357/aaa6d8. arXiv: 1706.01277 [astro-ph.HE].

[68] A. U. Abeysekara et al. “A Search for Dark Matter in the Galactic Halo with HAWC”. In: *JCAP* 02 (Feb. 23, 2018), p. 049. DOI: 10.1088/1475-7516/2018/02/049. arXiv: 1710.10288 [astro-ph.HE].

[69] Megan Longo Proper, J. Patrick Harding, and Brenda Dingus. “First Limits on the Dark Matter Cross Section with the HAWC Observatory”. In: *PoS* ICRC2015 (July 21, 2015). Ed. by Monica Tecchio and Daniel Levin, p. 1213. DOI: 10.22323/1.236.1213. arXiv: 1508.04470 [astro-ph.HE].

[70] J. Patrick Harding and Brenda Dingus. “Dark Matter Annihilation and Decay Searches with the High Altitude Water Cherenkov (HAWC) Observatory”. In: *PoS* ICRC2015 (July 13, 2015), p. 1227. DOI: 10.22323/1.236.1227. arXiv: 1508.04352 [astro-ph.HE].

[71] Fermi-LAT Collaboration. “Searching for Dark Matter Annihilation from Milky Way Dwarf Spheroidal Galaxies with Six Years of Fermi-LAT Data”. In: *Physical Review Letters* 115.23 (Nov. 30, 2015), p. 231301. DOI: 10.1103/PhysRevLett.115.231301. arXiv: 1503.02641 [astro-ph.HE].

[72] The Fermi-LAT Collaboration. "Updated Search for Spectral Lines from Galactic Dark Matter Interactions with Pass 8 Data from the Fermi Large Area Telescope". In: *Physical Review D* 91.12 (June 22, 2015), p. 122002. DOI: 10.1103/PhysRevD.91.122002. arXiv: 1506.00013 [astro-ph.HE].

[73] M. Ackermann et al. "Fermi LAT Search for Dark Matter in Gamma-ray Lines and the Inclusive Photon Spectrum". In: *Phys. Rev. D* 86 (2012), p. 022002. DOI: 10.1103/PhysRevD.86.022002. arXiv: 1205.2739 [astro-ph.HE].

[74] A. A. Abdo et al. "Constraints on Cosmological Dark Matter Annihilation from the Fermi-LAT Isotropic Diffuse Gamma-Ray Measurement". In: *JCAP* 04 (2010), p. 014. DOI: 10.1088/1475-7516/2010/04/014. arXiv: 1002.4415 [astro-ph.CO].

[75] Meng Su, Tracy R. Slatyer, and Douglas P. Finkbeiner. "Giant Gamma-ray Bubbles from Fermi-LAT: AGN Activity or Bipolar Galactic Wind?" In: *Astrophys. J.* 724 (2010), pp. 1044–1082. DOI: 10.1088/0004-637X/724/2/1044. arXiv: 1005.5480 [astro-ph.HE].

[76] M. G. Aartsen et al. "Search for Annihilating Dark Matter in the Sun with 3 Years of IceCube Data". In: *Eur. Phys. J. C* 77.3 (Mar. 8, 2017), p. 146. DOI: 10.1140/epjc/s10052-017-4689-9. arXiv: 1612.05949 [astro-ph.HE].

[77] M. G. Aartsen et al. "Search for Dark Matter Annihilations in the Sun with the 79-String IceCube Detector". In: *Phys. Rev. Lett.* 110.13 (Mar. 28, 2013), p. 131302. DOI: 10.1103/PhysRevLett.110.131302. arXiv: 1212.4097 [astro-ph.HE].

[78] A. Albert et al. "Search for Dark Matter Annihilation in the Earth Using the ANTARES Neutrino Telescope". In: *Phys. Dark Univ.* 16 (June 2017), pp. 41–48. DOI: 10.1016/j.dark.2017.04.005. arXiv: 1612.06792 [hep-ex].

[79] S. Adrián-Martínez et al. "A Search for Secluded Dark Matter in the Sun with the ANTARES Neutrino Telescope". In: *Journal of Cosmology and Astroparticle Physics* 05.05 (May 5, 2016), p. 016. DOI: 10.1088/1475-7516/2016/05/016. arXiv: 1602.07000 [hep-ex].

[80] S. Adrian-Martinez, A. Albert, M. Andre, et al. "Limits on Dark Matter Annihilation in the Sun Using the ANTARES Neutrino Telescope". In: *Physics Letters B* 759 (Aug. 10, 2016), pp. 69–74. DOI: 10.1016/j.physletb.2016.05.019. arXiv: 1603.02228 [astro-ph.HE].

[81] The Super-Kamiokande Collaboration et al. "Search for Neutrinos from Annihilation of Captured Low-Mass Dark Matter Particles in the Sun by Super-Kamiokande". In: *Phys. Rev. Lett.* 114.14 (Apr. 6, 2015), p. 141301. DOI: 10.1103/PhysRevLett.114.141301. arXiv: 1503.04858 [hep-ex].

[82] S. Desai et al. "Search for Dark Matter WIMPs Using Upward Through-Going Muons in Super-Kamiokande". In: *Phys. Rev. D* 70 (2004), p. 083523. DOI: 10.1103/PhysRevD.70.083523. arXiv: hep-ex/0404025.

[83] Jonathan L. Feng et al. "Testing the Dark Matter Interpretation of the DAMA/LIBRA Result with Super-Kamiokande". In: *JCAP* 01 (2009), p. 032. DOI: 10.1088/1475-7516/2009/01/032. arXiv: 0808.4151 [hep-ph].

[84] Nicole F. Bell, Matthew J. Dolan, and Sandra Robles. "Searching for Sub-GeV Dark Matter in the Galactic Centre Using Hyper-Kamiokande". In: *JCAP* 09 (Sept. 8, 2020), p. 019. DOI: 10.1088/1475-7516/2020/09/019. arXiv: 2005.01950 [hep-ph].

[85] Nicole F. Bell, Matthew J. Dolan, and Sandra Robles. "Searching for Dark Matter in the Sun Using Hyper-Kamiokande". In: *JCAP* 11 (Nov. 5, 2021), p. 004. DOI: 10.1088/1475-7516/2021/11/004. arXiv: 2107.04216 [hep-ph].

[86] Nicole F. Bell, Matthew J. Dolan, and Sandra Robles. "Dark Matter Pollution in the Diffuse Supernova Neutrino Background". In: *JCAP* 11 (Nov. 30, 2022), p. 060. DOI: 10.1088/1475-7516/2022/11/060. arXiv: 2205.14123 [hep-ph].

[87] Tarso Franarin, Malcolm Fairbairn, and Jonathan H. Davis. "JUNO Sensitivity to Resonant Absorption of Galactic Supernova Neutrinos by Dark Matter". In: *arXiv:1806.05015 [hep-ph]* (June 2018). arXiv: 1806.05015 [hep-ph].

[88] Gaëlle Giesen et al. "AMS-02 Antiprotons, at Last! Secondary Astrophysical Component and Immediate Implications for Dark Matter". In: *JCAP* 09 (Sept. 8, 2015), p. 023. DOI: 10.1088/1475-7516/2015/9/023. arXiv: 1504.04276 [astro-ph.HE].

[89] Lars Bergstrom et al. "New Limits on Dark Matter Annihilation from AMS Cosmic Ray Positron Data". In: *Phys. Rev. Lett.* 111 (Oct. 21, 2013), p. 171101. DOI: 10.1103/PhysRevLett.111.171101. arXiv: 1306.3983 [astro-ph.HE].

[90] Seyda Ipek, David McKeen, and Ann E. Nelson. "A Renormalizable Model for the Galactic Center Gamma Ray Excess from Dark Matter Annihilation". In: *Phys. Rev. D* 90.5 (Sept. 22, 2014), p. 055021. DOI: 10.1103/PhysRevD.90.055021. arXiv: 1404.3716 [hep-ph].

[91] M. Ackermann et al. "The Fermi Galactic Center GeV Excess and Implications for Dark Matter". In: *Astrophys. J.* 840.1 (May 4, 2017), p. 43. DOI: 10.3847/1538-4357/aa6cab. arXiv: 1704.03910 [astro-ph.HE].

[92] V. Bonnivard et al. “Dark Matter Annihilation and Decay in Dwarf Spheroidal Galaxies: The Classical and Ultrafaint dSphs”. In: *Mon. Not. Roy. Astron. Soc.* 453.1 (Oct. 11, 2015), pp. 849–867. DOI: 10.1093/mnras/stv1601. arXiv: 1504.02048 [astro-ph.HE].

[93] Haipeng An, Maxim Pospelov, and Josef Pradler. “New Stellar Constraints on Dark Photons”. In: *Phys. Lett. B* 725 (Oct. 1, 2013), pp. 190–195. DOI: 10.1016/j.physletb.2013.07.008. arXiv: 1302.3884 [hep-ph].

[94] Matthew J. Dolan, Frederick J. Hiskens, and Raymond R. Volkas. “Advancing Globular Cluster Constraints on the Axion-Photon Coupling”. In: *JCAP* 10 (Oct. 31, 2022), p. 096. DOI: 10.1088/1475-7516/2022/10/096. arXiv: 2207.03102 [hep-ph].

[95] Matthew J. Dolan, Frederick J. Hiskens, and Raymond R. Volkas. “Constraining Dark Photons with Self-consistent Simulations of Globular Cluster Stars”. In: *arXiv:2306.13335 [hep-ph]* (June 2023). arXiv: 2306.13335 [hep-ph].

[96] W. H. Press and D. N. Spergel. “Capture by the Sun of a Galactic Population of Weakly Interacting, Massive Particles”. In: *The Astrophysical Journal* 296 (1985), pp. 679–684. DOI: 10.1086/163485.

[97] Andrew Gould. “Weakly Interacting Massive Particle Distribution in and Evaporation from the Sun”. In: *The Astrophysical Journal* 321 (1987), p. 560. DOI: 10.1086/165652.

[98] Andrew Gould. “Resonant Enhancements in WIMP Capture by the Earth”. In: *Astrophys. J.* 321 (1987), p. 571. DOI: 10.1086/165653.

[99] Giorgio Busoni et al. “Evaporation and Scattering of Momentum- and Velocity-Dependent Dark Matter in the Sun”. In: *Journal of Cosmology and Astroparticle Physics* 10.10 (Oct. 23, 2017), p. 037. DOI: 10.1088/1475-7516/2017/10/037. arXiv: 1703.07784 [hep-ph].

[100] Andrew Gould. “Big Bang Archeology: WIMP Capture by the Earth at Finite Optical Depth”. In: *Astrophys. J.* 387 (1992), p. 21. DOI: 10.1086/171057.

[101] Raghuveer Garani and Sergio Palomares-Ruiz. “Dark Matter in the Sun: Scattering off Electrons vs Nucleons”. In: *JCAP* 05 (May 3, 2017), p. 007. DOI: 10.1088/1475-7516/2017/05/007. arXiv: 1702.02768 [hep-ph].

[102] Joseph Bramante, Antonio Delgado, and Adam Martin. “Multiscatter Stellar Capture of Dark Matter”. In: *Phys. Rev. D* 96.6 (Sept. 6, 2017), p. 063002. DOI: 10.1103/PhysRevD.96.063002. arXiv: 1703.04043 [hep-ph].

[103] Daniel T. Cumberbatch et al. “Light WIMPs in the Sun: Constraints from Helioseismology”. In: *Physical Review D* 82.10 (2010), p. 103503. DOI: 10.1103/PhysRevD.82.103503. arXiv: 1005.5102 [astro-ph.SR].

[104] Aaron C. Vincent and Pat Scott. “Thermal Conduction by Dark Matter with Velocity and Momentum-Dependent Cross-Sections”. In: *Journal of Cosmology and Astroparticle Physics* 04.04 (Apr. 22, 2014), p. 019. DOI: 10.1088/1475-7516/2014/04/019. arXiv: 1311.2074 [astro-ph.CO].

[105] Aaron C. Vincent, Aldo Serenelli, and Pat Scott. “Generalised Form Factor Dark Matter in the Sun”. In: *Journal of Cosmology and Astroparticle Physics* 08.08 (Aug. 19, 2015), p. 040. DOI: 10.1088/1475-7516/2015/08/040. arXiv: 1504.04378 [hep-ph].

[106] The Super-Kamiokande Collaboration et al. “An Indirect Search for WIMPs in the Sun Using 3109.6 Days of Upward-Going Muons in Super-Kamiokande”. In: *The Astrophysical Journal* 742.2 (2011), p. 78. DOI: 10.1088/0004-637X/742/2/78. arXiv: 1108.3384 [astro-ph.HE].

[107] M. G. Aartsen et al. “Search for Annihilating Dark Matter in the Sun with 3 Years of IceCube Data”. In: *Eur. Phys. J.* C77.3 (2017), p. 146. DOI: 10.1140/epjc/s10052-019-6702-y,10.1140/epjc/s10052-017-4689-9. arXiv: 1612.05949 [astro-ph.HE].

[108] Brian Batell et al. “Solar Gamma Rays Powered by Secluded Dark Matter”. In: *Physical Review D* 81.7 (2010), p. 075004. DOI: 10.1103/PhysRevD.81.075004. arXiv: 0910.1567 [hep-ph].

[109] Philip Schuster, Natalia Toro, and Itay Yavin. “Terrestrial and Solar Limits on Long-Lived Particles in a Dark Sector”. In: *Physical Review D* 81.1 (2010), p. 016002. DOI: 10.1103/PhysRevD.81.016002. arXiv: 0910.1602 [hep-ph].

[110] Nicole F. Bell and Kalliopi Petraki. “Enhanced Neutrino Signals from Dark Matter Annihilation in the Sun via Metastable Mediators”. In: *Journal of Cosmology and Astroparticle Physics* 04.04 (2011), p. 003. DOI: 10.1088/1475-7516/2011/04/003. arXiv: 1102.2958 [hep-ph].

[111] Jonathan L. Feng, Jordan Smolinsky, and Philip Tanedo. “Dark Sunshine: Detecting Dark Matter through Dark Photons from the Sun”. In: *Physical Review D* 93.11 (June 28, 2016), p. 115036. DOI: 10.1103/PhysRevD.93.115036. arXiv: 1602.01465 [hep-ph].

[112] Rebecca K. Leane, Kenny C. Y. Ng, and John F. Beacom. “Powerful Solar Signatures of Long-Lived Dark Mediators”. In: *Physical Review D* 95.12 (June 29, 2017), p. 123016. DOI: 10.1103/PhysRevD.95.123016. arXiv: 1703.04629 [astro-ph.HE].

[113] Samuel D. McDermott, Hai-Bo Yu, and Kathryn M. Zurek. "Constraints on Scalar Asymmetric Dark Matter from Black Hole Formation in Neutron Stars". In: *Phys. Rev. D* 85 (2012), p. 023519. DOI: 10.1103/PhysRevD.85.023519. arXiv: 1103.5472 [hep-ph].

[114] Chris Kouvaris and Peter Tinyakov. "Excluding Light Asymmetric Bosonic Dark Matter". In: *Phys. Rev. Lett.* 107 (2011), p. 091301. DOI: 10.1103/PhysRevLett.107.091301. arXiv: 1104.0382 [astro-ph.CO].

[115] Tolga Güver et al. "On the Capture of Dark Matter by Neutron Stars". In: *JCAP* 05 (May 13, 2014), p. 013. DOI: 10.1088/1475-7516/2014/05/013. arXiv: 1201.2400 [hep-ph].

[116] Raghuveer Garani, Yoann Genolini, and Thomas Hambye. "New Analysis of Neutron Star Constraints on Asymmetric Dark Matter". In: *JCAP* 05 (May 21, 2019), p. 035. DOI: 10.1088/1475-7516/2019/05/035. arXiv: 1812.08773 [hep-ph].

[117] Joseph Bramante et al. "Bounds on Self-Interacting Fermion Dark Matter from Observations of Old Neutron Stars". In: *Phys. Rev. D* 89.1 (Jan. 21, 2014), p. 015010. DOI: 10.1103/PhysRevD.89.015010. arXiv: 1310.3509 [hep-ph].

[118] Bridget Bertoni, Ann E. Nelson, and Sanjay Reddy. "Dark Matter Thermalization in Neutron Stars". In: *Phys. Rev. D* 88 (Dec. 3, 2013), p. 123505. DOI: 10.1103/PhysRevD.88.123505. arXiv: 1309.1721 [hep-ph].

[119] Nicole F. Bell, Andrew Melatos, and Kalliopi Petraki. "Realistic Neutron Star Constraints on Bosonic Asymmetric Dark Matter". In: *Phys. Rev. D* 87.12 (June 7, 2013), p. 123507. DOI: 10.1103/PhysRevD.87.123507. arXiv: 1301.6811 [hep-ph].

[120] Joseph Bramante, Tim Linden, and Yu-Dai Tsai. "Searching for Dark Matter with Neutron Star Mergers and Quiet Kilonovae". In: *Physical Review D* 97.5 (Mar. 12, 2018), p. 055016. DOI: 10.1103/PhysRevD.97.055016. arXiv: 1706.00001 [hep-ph].

[121] John Ellis et al. "Search for Dark Matter Effects on Gravitational Signals from Neutron Star Mergers". In: *Physics Letters B* 781 (June 10, 2018), pp. 607–610. DOI: 10.1016/j.physletb.2018.04.048. arXiv: 1710.05540 [astro-ph.CO].

[122] John Ellis et al. "Dark Matter Effects On Neutron Star Properties". In: *Physical Review D* 97.12 (June 15, 2018), p. 123007. DOI: 10.1103/PhysRevD.97.123007. arXiv: 1804.01418 [astro-ph.CO].

[123] Ann Nelson, Sanjay Reddy, and Dake Zhou. "Dark Halos around Neutron Stars and Gravitational Waves". In: *Journal of Cosmology and Astroparticle Physics* 07.07 (July 4, 2019), p. 012. DOI: 10.1088/1475-7516/2019/07/012. arXiv: 1803.03266 [hep-ph].

[124] Heinrich Steigerwald et al. "Dark Matter Thermonuclear Supernova Ignition". In: *arXiv:1912.12417 [astro-ph.HE]* (Dec. 2019). arXiv: 1912.12417 [astro-ph.HE].

[125] Grigoris Panotopoulos and Ilídio Lopes. "Constraints on Light Dark Matter Particles Using White Dwarf Stars". In: *International Journal of Modern Physics D* 29.08 (June 3, 2020), p. 2050058. DOI: 10.1142/S0218271820500583. arXiv: 2005.11563 [hep-ph].

[126] Matthew McCullough and Malcolm Fairbairn. "Capture of Inelastic Dark Matter in White Dwarves". In: *Physical Review D* 81.8 (2010), p. 083520. DOI: 10.1103/PhysRevD.81.083520. arXiv: 1001.2737 [hep-ph].

[127] Dan Hooper et al. "Inelastic Dark Matter As An Efficient Fuel For Compact Stars". In: *Physical Review D* 81.10 (2010), p. 103531. DOI: 10.1103/PhysRevD.81.103531. arXiv: 1002.0005 [hep-ph].

[128] Joseph Bramante. "Dark Matter Ignition of Type Ia Supernovae". In: *Phys. Rev. Lett.* 115.14 (Sept. 29, 2015), p. 141301. DOI: 10.1103/PhysRevLett.115.141301. arXiv: 1505.07464 [hep-ph].

[129] Gianfranco Bertone and Malcolm Fairbairn. "Compact Stars as Dark Matter Probes". In: *Physical Review D* 77.4 (2008), p. 043515. DOI: 10.1103/PhysRevD.77.043515. arXiv: 0709.1485 [astro-ph].

[130] Nirmal Raj, Philip Tanedo, and Hai-Bo Yu. "Neutron Stars at the Dark Matter Direct Detection Frontier". In: *Physical Review D* 97.4 (Feb. 10, 2018), p. 043006. DOI: 10.1103/PhysRevD.97.043006. arXiv: 1707.09442 [hep-ph].

[131] Masha Baryakhtar et al. "Dark Kinetic Heating of Neutron Stars and An Infrared Window On WIMPs, SIMPs, and Pure Higgsinos". In: *Physical Review Letters* 119.13 (Sept. 26, 2017), p. 131801. DOI: 10.1103/PhysRevLett.119.131801. arXiv: 1704.01577 [hep-ph].

[132] Nicole F. Bell, Giorgio Busoni, and Sandra Robles. "Heating up Neutron Stars with Inelastic Dark Matter". In: *JCAP* 09 (Sept. 10, 2018), p. 018. DOI: 10.1088/1475-7516/2018/09/018. arXiv: 1807.02840 [hep-ph].

[133] Aniket Joglekar et al. "Relativistic Capture of Dark Matter by Electrons in Neutron Stars". In: *Phys. Lett. B* 809 (Sept. 4, 2020), p. 135767. DOI: 10.1016/j.physletb.2020.135767. arXiv: 1911.13293 [hep-ph].

[134] Javier F. Acevedo et al. "Warming Nuclear Pasta with Dark Matter: Kinetic and Annihilation Heating of Neutron Star Crusts". In: *JCAP* 03 (Mar. 17, 2020), p. 038. DOI: 10.1088/1475-7516/2020/03/038. arXiv: 1911.06334 [hep-ph].

[135] Nicole F. Bell, Giorgio Busoni, and Sandra Robles. "Capture of Leptophilic Dark Matter in Neutron Stars". In: *JCAP* 06 (June 28, 2019), p. 054. DOI: 10.1088/1475-7516/2019/06/054. arXiv: 1904.09803 [hep-ph].

[136] Raghuveer Garani and Julian Heeck. "Dark Matter Interactions with Muons in Neutron Stars". In: *Phys. Rev. D* 100.3 (Aug. 31, 2019), p. 035039. DOI: 10.1103/PhysRevD.100.035039. arXiv: 1906.10145 [hep-ph].

[137] Shiuli Chatterjee et al. "Faint Light of Old Neutron Stars and Detectability at the James Webb Space Telescope". In: *Phys. Rev. D* 108.2 (July 11, 2023), p. L021301. DOI: 10.1103/PhysRevD.108.L021301. arXiv: 2205.05048 [astro-ph.HE].